



Long-Duration Exposure Criteria for Head-Supported Mass

By

Barclay P. Butler

and

Nabih M. Alem

Aircrew Protection Division

DNIC QUALITY INSPECTED 4

19970929 056

August 1997

Approved for public release, distribution unlimited.

U.S. Army Aeromedical Research Laboratory
Fort Rucker, Alabama 36362-0577

Notice

Qualified requesters

Qualified requesters may obtain copies from the Defense Technical Information Center (DTIC), Cameron Station, Alexandria, Virginia 22314. Orders will be expedited if placed through the librarian or other person designated to request documents from DTIC.

Change of address

Organizations receiving reports from the U.S. Army Aeromedical Research Laboratory on automatic mailing lists should confirm correct address when corresponding about laboratory reports.

Disposition

Destroy this document when it is no longer needed. Do not return it to the originator.

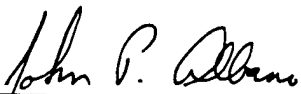
Disclaimer

The views, opinions, and/or findings contained in this report are those of the author(s) and should not be construed as an official Department of the Army position, policy, or decision, unless so designated by other official documentation. Citation of trade names in this report does not constitute an official Department of the Army endorsement or approval of the use of such commercial items.

Human use

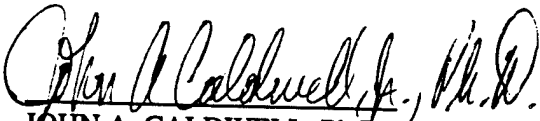
Human subjects participated in these studies after giving their free and informed voluntary consent. Investigators adhered to AR 70-25 and USAMRMC Reg 70-25 on Use of Volunteers in Research.

Reviewed:

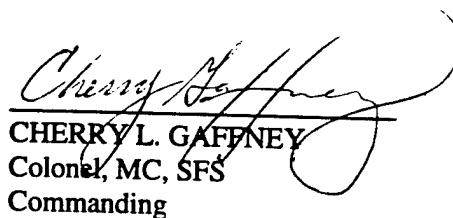


JOHN P. ALBANO
MAJ, MC, SFS
Director, Aircrew Protection
Division

Released for publication:



JOHN A. CALDWELL, Ph.D.
Chairman, Scientific
Review Committee



CHERYLL L. GAFFNEY
Colonel, MC, SFS
Commanding

REPORT DOCUMENTATION PAGE

1a. REPORT SECURITY CLASSIFICATION Unclassified		1b. RESTRICTIVE MARKINGS .													
2a. SECURITY CLASSIFICATION AUTHORITY		3. DISTRIBUTION / AVAILABILITY OF REPORT Approved for public release; distribution unlimited													
2b. DECLASSIFICATION / DOWNGRADING SCHEDULE															
4. PERFORMING ORGANIZATION REPORT NUMBER(S) USAARL Report No. 97-34		5. MONITORING ORGANIZATION REPORT NUMBER(S)													
6a. NAME OF PERFORMING ORGANIZATION U.S. Army Aeromedical Research Laboratory	6b. OFFICE SYMBOL <i>(If applicable)</i> MCMR-UAD	7a. NAME OF MONITORING ORGANIZATION U.S. Army Medical Research and Materiel Command													
6c. ADDRESS (City, State, and ZIP Code) P.O. Box 620577 Fort Rucker, AL 36362-0577		7b. ADDRESS (City, State, and ZIP Code) 504 Scott Street Fort Detrick, MD 21702-5012													
8a. NAME OF FUNDING / SPONSORING ORGANIZATION	8b. OFFICE SYMBOL <i>(If applicable)</i>	9. PROCUREMENT INSTRUMENT IDENTIFICATION NUMBER													
8c. ADDRESS (City, State, and ZIP Code)		10. SOURCE OF FUNDING NUMBERS <table border="1" style="width:100%; border-collapse: collapse; margin-top: 5px;"> <thead> <tr> <th style="width:25%;">PROGRAM ELEMENT NO.</th> <th style="width:25%;">PROJECT NO.</th> <th style="width:15%;">TASK NO.</th> <th style="width:35%;">WORK UNIT ACCESSION NO.</th> </tr> </thead> <tbody> <tr> <td>62787A</td> <td>30162787A878</td> <td>EB</td> <td>DA320693</td> </tr> </tbody> </table>		PROGRAM ELEMENT NO.	PROJECT NO.	TASK NO.	WORK UNIT ACCESSION NO.	62787A	30162787A878	EB	DA320693				
PROGRAM ELEMENT NO.	PROJECT NO.	TASK NO.	WORK UNIT ACCESSION NO.												
62787A	30162787A878	EB	DA320693												
11. TITLE (Include Security Classification) Long-duration exposure criteria for head-supported mass (U)															
12. PERSONAL AUTHOR(S) Barclay P. Butler and Nabih M. Alem															
13a. TYPE OF REPORT Final	13b. TIME COVERED FROM TO	14. DATE OF REPORT (Year, Month, Day) 1997 August	15. PAGE COUNT 52												
16. SUPPLEMENTAL NOTATION															
17. COSATI CODES <table border="1" style="width:100%; border-collapse: collapse; margin-top: 5px;"> <thead> <tr> <th style="width:33%;">FIELD</th> <th style="width:33%;">GROUP</th> <th style="width:33%;">SUB-GROUP</th> </tr> </thead> <tbody> <tr><td> </td><td> </td><td> </td></tr> <tr><td> </td><td> </td><td> </td></tr> <tr><td> </td><td> </td><td> </td></tr> </tbody> </table>		FIELD	GROUP	SUB-GROUP										18. SUBJECT TERMS (Continue on reverse if necessary and identify by block number) head-supported mass, repeated impact, helmet, whole-body vibration	
FIELD	GROUP	SUB-GROUP													
19. ABSTRACT (Continue on reverse if necessary and identify by block number) <p>The modern crew station of Army helicopters uses the helmet as an integral component of the aircraft control systems. What was once viewed as a simple device for crash protection now supports devices including night vision goggles, chemical mask, head-up displays, and weapon aiming systems. These devices combine to increase the biomechanical stress in the neck. This study investigated the effects of increasing helmet torque on the motion of the helmeted head under the conditions of long-duration whole-body vibration exposure.</p> <p>Twelve U.S. Army volunteer aviators were exposed to 4 hours of whole-body vibration, similar to that found in a UH-60 helicopter, while wearing four different helmets. Helmet torques, as calculated at the point where the head connects to the spine, ranged from a standard aviator helmet to a helmet with a chemical mask and a night vision goggle. Head motion was measured using a three dimensional active infrared marker system attached to a fixture held in the subject's teeth.</p> <p style="text-align: right;">(continued on next page)</p>															
20. DISTRIBUTION / AVAILABILITY OF ABSTRACT <input checked="" type="checkbox"/> UNCLASSIFIED/UNLIMITED <input type="checkbox"/> SAME AS RPT. <input type="checkbox"/> DTIC USERS		21. ABSTRACT SECURITY CLASSIFICATION Unclassified													
22a. NAME OF RESPONSIBLE INDIVIDUAL Chief, Science Support Center		22b. TELEPHONE (Include Area Code) (334) 255-6907	22c. OFFICE SYMBOL MCMR-UAX-SI												

Acknowledgments

The authors wish to acknowledge the efforts of the following personnel for their efforts in generating the human response data used for this report:

SSG Brad Erickson was responsible for managing the technicians during the data acquisition phase. He was able to keep three separate primary investigators satisfied, all whom wanted data from different aspects of the experiment. SSG Erickson also was helpful in digging up the bits and pieces of information that are invariably required to complete the writing for any research effort.

Mr. Al Lewis, the senior design engineer for this project, was responsible for designing and implementing the control system managing the data acquisition. His management of his staff to provide technical operators for the multiaxis ride simulator allowed us to complete this effort in the most efficient manner.

Finally, SPC Rene Guerrero and Mrs. Mary Gramling worked diligently at reformatting the initial manuscript into standard USAARL format. Their work is gratefully acknowledged.

Without these people, this project would never have materialized.

Table of contents

	<u>Page</u>
Introduction	1
Study significance	3
Biomechanics of whole-body vibration exposure	4
Skeletal muscle response to whole-body vibration exposure	5
Head motion due to whole-body vibration exposure	5
Research methodology	6
Helmet loads	11
Subject grouping and helmet rotation	11
Instrumentation	12
Data analysis	13
Assumptions	16
Analysis	17
Discussion	20
Conclusions	24
Recommendations	24
References	25

Table of contents (continued)

	<u>Page</u>
Appendices	
A. Subject briefing	39
B. Medical screening form	42
C. Multiaxis ride simulator	44
D. Statistical tables	46
E. Glossary	50
F. List of abbreviations	52

List of figures

1. Force vectors.	27
2. Force vector rotation.	27
3. Head frame of reference	28
4. Short-duration head pitch response.	28
5. Short-duration helmet torque	29
6. Long-duration helmet torque	29
7. Marker location for the bite bar.	30
8. Bite bar coordinates.	30
9. Bite bar geometry.	31
10. Signal analysis flow chart.	31
11. Head pitch motion.	32
12. Head X motion.	32
13. Head Z motion.	33

Table of contents (continued)

Page

List of figures (continued)

14. Head pitch peaks for 16 epochs	33
15. Peak head pitch versus time, helmet 1	34
16. Peak head pitch versus time, helmet 2	34
17. Peak head pitch versus time, helmet 3	35
18. Peak head pitch versus time, helmet 4	35
19. Average peak head pitch motion versus time	36
20. Average peak head X motion versus time	36
21. Average peak head Z motion versus time	37
22. Average peak head pitch motion	37
23. Average peak head X motion	38
24. Average peak head Z motion	38

List of tables

1. Helmet description with weight moments	12
2. Helmet configuration and subject grouping	12
3. Tukey test for helmet at each epoch	19
4. Tukey test for helmets	20

Introduction

The modern crew station of U.S. Army helicopters uses the helmet as an integral component of the aircraft control systems. What was once viewed as a simple device for crash protection, the helmet has evolved into an equipment mounting platform. Aviator helmets now support numerous combinations of devices including night vision goggles (NVGs), chemical mask, oxygen system, head-up display (HUD), forward looking infrared (FLIR) display, flash blindness and laser eye protection, and weapon aiming systems. All these devices add to the weight of the helmet, which in turn contribute to increased biomechanical stress in the muscles of the neck that are responsible for controlling head motion.

Helmet weight can be characterized by its mass and center of mass. Mass is a concept that describes an object's resistance to acceleration and is proportional to an object's weight (Beer and Johnston, 1988). The higher the mass of an object the greater the resistance the object has to acceleration. An object's center of mass is a concept that describes the single location, or point in space, where all of the moments acting on the object sum to zero (McGill and King, 1989). Conceptually, this is similar to the idea of balancing an object on a knife-edge. Here, the forces that attempt to rotate the object in one direction are counterbalanced by the forces that attempt to rotate it in the other direction. The concept of center of mass extends this idea to three dimensions and uses forces and moments in all directions, not just in the direction of gravity.

The helmet mass and center of mass combine to create a torque that must be counterbalanced by the muscles in the back of the neck to maintain an upright posture. The head, too, creates a torque that attempts to rotate the head, moving the chin downward towards the chest. The torques from the helmet and the head combine to create a torque that is larger than the torque due to the head alone. The pivot point through which this torque operates is on top of the cervical spine and is known as the atlanto-occipital (AO) complex (Sobotta, 1990). Figure 1 shows the head, the location of the AO complex on top of the cervical spine, and the locations of the head center of mass and the helmet center of mass. Force vectors also are shown located at each center of mass. These force vectors must be counterbalanced by the muscles in the back, or posterior, of the neck.

The amount of torque that must be counterbalanced by the posterior neck muscles depends on the mass of the head and helmet and on the distance these centers of mass are from the AO complex. Head mass is considered a constant at about 4.2 kg. Helmet mass, however, can change, either from the introduction of new helmet designs, or more readily, through the attachment of devices to the helmet itself. These devices, such as those mentioned above, are typically added to the front of the helmet to aid in vision, filter air, or add ballistic or eye protection, just to name a few. The masses of these devices also add to the helmet and head mass resulting in another increase in torque around the AO complex. This situation can continue to progress to a point where the total head-supported mass creates a torque that is more than the posterior neck muscles can effectively control.

The total head-supported mass is not the only factor affecting the stress on the posterior neck muscles. Changes in head posture can change the effective length of the lever arm connecting the helmet center of mass to the AO complex as initially shown in figure 1. For example, by rotating the head so the face points upwards, the force vectors are moved towards, and sometimes past, the AO complex (figure 2). This reduces the torque that the neck muscles must support.

The presence of whole-body vibration (WBV), as is always true in a helicopter, causes the head to pitch up and down (Paddan and Griffin, 1988). This pitching motion causes an involuntary stretch response in the posterior muscles of the neck that further increases the amount of force produced by these muscles. The duration of a helicopter flight requires the posterior muscles of the neck to exert counterbalancing forces for a greater period of time than required under more natural conditions. These factors affect the amount of biomechanical stress experienced by the posterior neck muscles, and play a role in determining a reasonable head-supported mass limit for Army rotary-wing aviators.

The identification of a limit for head-supported mass was a topic of research undertaken at the U.S. Army Aeromedical Research Laboratory (USAARL), Fort Rucker, Alabama (Butler, 1992). In this study, volunteer aviators were exposed to different helmet torques while experiencing simulated UH-60 helicopter vibration for 20-minute periods. Results showed that the motion of the combined head and helmet was not different from the motion of the head alone when the total head-supported torque was less than 90 Newton-centimeters (N·cm) measured relative to the AO complex. The practical application of these results indicates that using the modern NVG with the batteries as a counterbalance is satisfactory, but flying with a chemical mask will stress the posterior neck muscles. While this is a significant first step in specifying limits for head-supported mass, there is a need to extend this criterion to be applicable for longer duration exposures (4 hours) that more nearly approach actual operational flight times experienced by Army rotary-wing aviators.

In 1991, USAARL researchers completed the data acquisition phase of experiments addressing head-supported mass under long-duration WBV exposure (Butler, Lantz, and Alem, 1991). This report will use the experimental results from that study to test the hypothesis that under simulated UH-60 helicopter WBV, there will be no change in head motion resulting from either (a) exposure duration, or (b) the magnitude of the head-supported mass. It is the purpose of this report to perform this analysis, apply the results to the initial head-supported mass criteria, and develop a more robust helmet design recommended practice for Army aviation.

Study significance

Limitations and delimitations

The primary limitations of this study involved the desire to maintain a high level of subject safety by minimizing the exposure time to large magnitude head-supported mass under WBV conditions. As such, only 12 subjects were incorporated into the study, and exposure durations were limited to 4 hours for any one session. A secondary limitation was the inability to analyze the electromyographic data from the posterior neck muscles. The electromyographic data would have been useful in determining the presence of muscle fatigue both over time and as a result of the magnitude of head-supported mass.

The delimitations of this study necessarily arose out of a desire to obtain reliable results with as small a subject pool as was practical. One method of achieving these results was to use a homogenous subject population. As a result of this approach, this study did not address head-supported mass for female aviators, nor did it address the very large or very small male aviator. Also, in-flight biomechanical performance was not assessed, nor was aviator flight maneuver performance, cognitive performance, or other psychophysical performance characteristics.

Literature review

The literature supporting this research effort falls into two broad and separate areas: (1) studies involving acute and chronic exposure effects of WBV, and (2) studies involving head motion during impact events similar to that experienced during automobile crashes. The area addressing WBV exposure effects is further split into two subareas. The first of these addresses the biomechanical effects of WBV exposure. This area is interesting in that it lays the groundwork for understanding vibration transfer to the head and neck. It also sets the stage for understanding acute effects of WBV with specific applications to skeletal muscle responses. However, there are only a few studies that actually address head motion under WBV, and only one that addresses helmeted head motion in this environment. The studies involving chronic exposure to WBV are geared to understanding disease effects. These have little applicability to this effort and, therefore, will not be addressed.

The second body of literature involves head impact studies. These are most useful in showing just what WBV exposure is not. For example, head motion arising from an automobile crash occurs so rapidly that there is no time for even reflexive neck muscle responses (Chaffin and Anderson, 1984). In contrast, head motion arising from WBV involves relatively static responses where the muscles of the neck are actively involved in maintaining posture and in reacting to vibration disturbances. Nevertheless, this body of work was pioneering in developing the instrumentation used in head motion studies. Therefore, it will be cited in the research methodology section of this report to refer to specific instrumentation procedures.

Biomechanics of whole-body vibration exposure

Early work in WBV began with testing geared toward discovering the nature of vibration transfer through the body (Guignard and Irving, 1960). Of particular interest was determining how much energy was absorbed by the body. Energy transfer measurements were made on inert devices to test for their vibration stability. To perform this measurement, first the source of the vibration was measured. This was known as the input vibration. Next, the result of the vibration transfer through the object was measured. This was the output vibration. The absorbed vibration was the difference between the input and output vibration levels. To perform these experiments on human subjects, volunteers were asked to sit on a seat attached to a vertical, or Z-axis, aligned platform that would vibrate back and forth in a sinusoidal fashion. Acceleration measurements were made using accelerometers attached to the hard underside of the seat pan to capture the input vibration, and from the top of the subject's head to capture the output vibration. The vibration platform was excited at discrete frequencies ranging from 2 to 40 cycles per second, or hertz (Hz). In calculating the transfer functions by dividing the output by the input, a dominant peak was found near 5 Hz with the output vibration nearly twice as large as the input vibration. This peak is an example of resonance, that is, a condition under which a cyclic input function results in an output that is larger than the input. This crude but effective technique set the stage for further refining whole-body resonant frequencies and for identifying resonant frequencies for body segments as well as specific organ systems.

These techniques were extended from single Z-axis measurements to multiple axis measurements at the head. The coordinate system for the head is shown in figure 3. Here the Z-axis, or the axially aligned axis, is oriented vertically with the positive axis oriented upwards. The X-axis is oriented front to back, or anterior to posterior (AP), with the positive axis aligned forward. The Y-axis is oriented laterally with the positive axis aligned to the left. These axes are aligned in a right-handed coordinate system. Figure 3 also shows the rotational axis of pitch, yaw, and roll.

Multiaxis vibration measurements of the head were first reported by Griffin for sinusoidal vertical vibration (Griffin, 1975). Griffin used linear accelerometers connected to a fixture, or bite bar, held between the teeth to measure head acceleration. He found that the predominant head vibration was in the Z-axis, followed by the X-axis, and then the Y-axis, the latter two showing less than 20 percent of the Z-axis vibration levels. These data indicated that the head moved in a vertical fashion for vertical input vibration. Considering that helicopter vibration is predominantly vertical, this would suggest that vertical head motion would be the most significant motion for the helmeted aviator.

In a subsequent effort, Griffin studied the effect of posture on vibration transmitted to the head (Griffin, 1975). He first asked the subject to sit in a posture that was most comfortable, and then sit in a posture where vibration transmitted to the body was the least comfortable. He showed that when subjects were in an upright posture with their spines aligned with the vibration axis, they reported the most uncomfortable condition. The most comfortable condition was

noted when their spines were far out of the vibration axis. It is interesting to note that the preferred UH-1 Huey pilot posture is leaning forward, not upright. This result also has implications for experimental studies indicating that posture must either be controlled or measured to account for variations in transmitted vibration.

Skeletal muscle response to whole-body vibration exposure

Interest arose in investigating the effects of vibration exposure on skeletal muscle response. Matthews began an investigation using isolated muscle preparations and applying vibrating probes directly to the stretched tendons (Matthews, 1972). He showed that sinusoidal vibration resulted in a sinusoidal electrical burst response in the muscle, indicating a contraction-coupling reaction that was synchronized with the vibration frequency. He also demonstrated that random vibration stimulation did not show the sinusoidal burst pattern, but rather a complex burst pattern again related to the vibration signal. He theorized that the stretch response in the muscle was dependent upon the velocity of the stretching, which was consistent with his experimental data. These results are interesting in that helicopter vibrations can be characterized as a set of sinusoids related to the frequency of the main rotor blade passing by a given point.

Wilder, and others, extended Matthews' isolated muscle work by studying electromyographic (EMG) signals--the electrical signals generated by muscles during contraction--from volunteer subjects exposed to sinusoidal vibration (Wilder et al., 1982). They placed sensing surface electrodes over the paraspinal muscles of the lower back and measured input vibration at the seat pan, and output vibration at the top of the head. They asked volunteer subjects to maintain different postural angles for 30-minute periods while exposed to sinusoidal WBV. They verified the results of Griffin (1975) that postural changes affected transmitted vibration, and also showed paraspinal muscle fatigue using measures of EMG median spectral shift. Their results indicated that vibration induces muscle fatigue more quickly than in a nonvibrated control group, and that muscle fatigue could be measured in a vibration environment using spectral analysis techniques on the EMG signals.

Head motion due to whole-body vibration exposure

Detailed studies of head motion under WBV began with Sandover in 1978. He combined the techniques of mounting an axially aligned accelerometer to a bite bar and to the top of the head. He showed that the two accelerometers yielded dramatically different levels of axial acceleration, with the bite bar accelerometer showing more axial vibration than the head-mounted accelerometer. He concluded that the pitch motion of the head had caused the apparently larger axial response from the bite bar accelerometer as compared to the head mounted accelerometer. These data suggest that the pitch motion of the head may be the dominant response to axial vibration, and axial head motion may be a secondary response. Also,

understanding the relationship between the location of the accelerometer (or other transducers) and the dynamics of the underlying motion is critical to obtaining accurate head motion results. Paddan and Griffin (1988) were the first to report multi-axis measurements of head motion due to vertical WBV. Using multiple accelerometers attached to a bite bar, they were able to capture all six axes of motion as shown in figure 3. Their results indicated that head pitch motion was the predominant vibration, followed by Z-axis motion, and then X-axis motion. Very little motion was seen in the Y, yaw, or roll axes. This indicates that axial vibration results in a planar response for head motion with the dominant motions being in the AP and SI translations and pitch rotation. That is, head motion is confined to the midsagittal plane, or a vertical plane lying between the eyes.

The head motion measuring techniques developed by Paddan and Griffin (1988) were employed by Butler to make detailed measurements of the helmeted aviator exposed to short duration sinusoidal Z-axis vibration (Butler, 1992). Using 12 different helmet configurations (three mass and four center-of-mass parameters), he showed that there were significant differences in head pitch acceleration when the weight moment of the helmet exceeded 90 N·cm of torque measured relative to the AO complex. Using EMG measurements of the trapezius muscle at the back of the neck, Butler also showed significant increases in myoelectric activity when the helmet exceeded this 90 N·cm criteria.

In summary, axial WBV, similar to that found in helicopters, results in head motion confined to the midsagittal plane. The predominant head motions are pitch rotation and AP and SI translations. Myoelectric responses from the posterior neck muscles show burst responses that are synchronized with the vibration response. Muscle fatigue is indicated when the myoelectric responses show median spectral frequency shifts to lower frequencies, and/or increases in myoelectric peak magnitudes.

Research methodology

Describing the effects of head-supported mass on aviator performance is a complex task requiring a multidisciplinary approach. In addressing this problem, we designed a research protocol investigating the effects of head-supported mass on head and neck biomechanics, neck muscle fatigue, head tracking performance, target acquisition performance, multitask performance, head ballistic motion, and levels of brain activity (Butler, Lantz, and Alem, 1991). This report documents only the biomechanics effort describing head motion as a result of exposure to varying helmet torques and exposure duration. Nevertheless, to more fully understand the experimental environment experienced by the subjects, it is necessary to describe the complete experimental protocol.

Prior to testing, it was necessary to select, screen, and train subjects for participation in the protocol. Subjects were recruited from aviators stationed at Fort Rucker, Alabama. They were solicited by advertisements published in the post bulletin, by visits to units on post during

training periods, and by word of mouth. The subject pool was then screened to obtain a homogeneous subject set reflective of the average aviator.

Subject selection was limited to male aviators only. This selection criterion was justified because this effort was considered a continuation of an earlier one defining short-duration effects of head-supported mass. Had females been included in this protocol, there would have been no baseline from which to compare long-duration exposure effects. Also, at the time the experimental data acquisition phase was performed, there simply were not enough female aviators on active duty, let alone stationed at Fort Rucker, to support a statistical study. More recently, however, a parallel research effort has been initiated investigating the effects of head-supported mass on female aviator performance.

The next selection criterion was subject stature and weight. Subjects were required to be at the 50th percentile male aviator stature (USAARL, 1988), ± 10 percent. Subjects also were required to have a weight that was proportional to stature, again, ± 10 percent. Finally, subjects were eliminated from the study if they participated in frequent NVG training (defined as more than one NVG training flight per week), or participated in any physical training exercises that specifically targeted strengthening of the neck muscles. This screening continued until 12 subjects were recruited.

Once the subjects met the selection criteria, they were briefed formally on the nature of their participation in the protocol. Of particular importance was ensuring the subjects understood that they would be required to undergo exposure to WBV while wearing four different weighted helmets. The WBV exposure would last for 4 hours, and would be repeated for each of the four helmets to complete the protocol. The complete briefing can be reviewed in appendix A.

Once the subjects were selected and briefed, each was screened by a medical monitor. This was required to ensure the subjects did not have any medical conditions that could be exacerbated by exposure to WBV or by wearing high-torque helmets. The medical screening form can be reviewed in appendix B. Flight surgeons assigned to the USAARL performed this screening, and later acted as medical monitors for the experimental phase of the protocol. These were required for safety during WBV exposure in the unlikely event of an accident involving the multiaxis ride simulator (MARS).

Prior to experimental runs, the subjects were familiarized with the experimental setup. Each subject was instrumented with all the apparatus that would be required during the data runs. First, subjects were fitted with a device called a bite bar that held three active infrared position markers. They were required to bite onto a horseshoe-shaped bite plate covered with dental impression material. This obtained an impression of their bite that was used to achieve the same registration of the bite bar for all experimental runs. A fixture holding the infrared markers was then attached to the dental impression. The entire device (the markers and the dental impression) was termed the bite bar.

The bite bar was used to capture the three dimensional position of the head. This was used later to calculate head pitch motion, X motion, and Z motion. Additionally, two infrared markers were attached to a fixture cemented to the skin over the sternum, and two were attached to another fixture cemented to the skin over the first thoracic vertebrae (T1). These captured the motion at the base of the neck: the input motion to the head-neck system. Finally, three markers were attached to the helmet itself, and three markers were attached to the UH-60 seat frame. The helmet markers were used to capture any slippage between the helmet and head by comparing helmet motion to head motion. The last set of three markers on the seat were used to capture seat input motion.

Next, subjects were instrumented with EMG electrodes placed around the circumference of the neck. Each consisted of an electrode pair arranged to record EMG signals in a differential mode. The differential recording allowed for the cancellation of electrical and mechanical noise that was common to each electrode in the pair, and only transduced electrical signals that were dissimilar across the electrode pair. The first set of electrodes was placed over the right and left trapezius muscles at the back of the neck. The next set was placed over the right and left splenius capitus muscles on the sides of the neck. The last were placed over the right and left sternocleidomastoid muscles at the front of the neck. All electrodes were placed at the level of the fourth cervical vertebrae, or the C4 level, positioned by palpating for the belly of the muscle, and aligned parallel to the long axis of the muscle. An EMG ground, used to ensure both electrical safety and EMG signal quality, was placed over the bony portion of the lower forearm just above the wrist.

Each subject was then asked to sit in a UH-60 seat placed on top of the MARS. The UH-60 seat, manufactured by Simula, Inc., was stiffened to reduce seat pitch by adding a center front leg. They belted themselves into the seat using only the crotch belt and the two lap belts. The shoulder straps were not used because they would interfere with the EMG electrodes around the neck when they voluntarily moved their heads.

For the neck muscle fatigue investigation, each subject was required to perform a neck muscle EMG calibration routine. The EMG calibrations were used to quantify the amount of effort he exerted for each helmet configuration. The procedure for head flexion calibration is described first. This routine began by placing a headband around the subject's head and attaching the headband to a tension load cell. This cell was attached to a fixed metal frame that encircled the head, and was connected to the headband using a small chain. His upright posture was maintained by adding or removing a number of links in the chain connecting the load cell to the head band. He then pulled in an isometric fashion against the load cell by attempting to flex the head forward. For the first three pulls he was asked to pull as hard as he could, for up to 2 seconds, and then release his effort. The largest of these three trials was considered his maximum voluntary contraction (MVC).

Next, EMG calibration routines were performed by asking the subject to match his pulling effort to increasing and decreasing target levels. He was shown a computer monitor screen with

a graph depicting two bars of a bar chart. One represented the tension on the load cell in the flexion direction. The other represented a target tension that the subject was supposed to match with his flexion effort. The target tension bar would cycle from 0 to 30 percent MVC and then return to 0 percent MVC at a rate of 2 percent MVC per second. This cycle took 30 seconds and was repeated three times. This completed the flexion calibration routine. The entire EMG calibration routine then was repeated for head extension efforts. Finally, the complete EMG calibration routine was repeated following the 4-hour test to capture any changes in neck muscle calibrations.

One final EMG calibration routine was performed prior to testing with vibration. First the subject sat in an upright posture without a helmet for 30 seconds while EMG data were captured. Then, he donned the experimental helmet loaded with the testing configuration of the day and sat in an upright posture for 30 seconds while EMG data were captured. This was done to assess the level of effort for the unloaded versus the loaded head, absent vibration.

The next step in the familiarization routine was to expose the subject to 15 minutes of WBV while he performed all of the testing procedures. For the actual testing, this basic 15-minute cycle was repeated 16 times to make up the total 4-hour exposure. For the familiarization trial, the subject wore a helmet with a torque magnitude of approximately the standard aviator helmet, the SPH-4B. The following tests were performed during the 15-minute epoch.

The first test of the 15-minute epoch was the biomechanics test. Here, the subject was asked to sit in a relaxed upright posture and face towards a target located at eye level at a distance of 80 inches toward their front. This lasted 1 minute. About 15 seconds into the test, a 15-second data acquisition window was activated capturing both EMG and position data. The instrumentation for the position measurements of the biomechanics test are fully described in the instrumentation section later in this section.

The second test of the 15-minute epoch was a 2-minute head tracking task. For this test, the subject was required to point a helmet-mounted columnated beam (a light spot) at a moving target 80 inches to the front. The target would move in a random walk motion at a rate of 4 degrees per second. The range of the target was plus or minus 35 degrees in azimuth, and plus or minus 15 degrees in elevation. The subject was required to keep the spot at the center of the target during the target motion. Errors were measured for X and Y deviations from the center of the target at a sampling rate of 20 Hz.

The third test of the 15-minute epoch was a 5-minute vigilance task used to assess target acquisition reaction times. Here, the subject was asked to monitor four red, light-emitting diodes (LEDs) located in a rectangular arrangement at the periphery of his visual perception. The LEDs flashed on in a random pattern and the subject was required to turn them off as fast as he could. A LED was turned off by having the subject point the head-mounted columnated beam at a photosensitive diode collocated with it. The time between the LED flash and his "hitting" it was

measured. Neck muscle EMG also was measured between LED-flash to LED-hit to capture the EMG effects of ballistic head motion.

The final task of the 15-minute epoch was the 7-minute synthetic work environment (SWE) task. This is thought to test a multitasking skill required in aviation. Because of the difficulty of this task, each subject was given 10 training sessions of 20 minutes each over at least 5 days. Performance scores were posted to encourage maximum efforts through competition.

For the SWE tests, the subject was required to perform four computer generated tasks simultaneously (appendix A). The first was a seven letter recognition task. Once having seen the target seven letters, he had to tell if a presented letter was or was not in the target list. If the response was correct, he earned points. If the response was wrong, he was assessed penalty points.

The second task involved auditory recognition. The subject was presented with one of two tones. If the tone was the high tone, he was to respond. If the tone was the low tone, he was to ignore it. He received points for correct responses and was penalized points for incorrect responses.

The third task was a three column addition task. The subject was required to add two numbers of three digits each. If he got the correct answer, he received points. Penalty points were assessed for incorrect answers.

The fourth task involved position discrimination. Here, the subject was required to let a moving bar drift towards one end of a predetermined and known interval. The closer he let the target bar get to the end before resetting the bar, the more points he would receive. If he let the bar touch the end, penalty points were assessed.

All the SWE tasks were performed simultaneously on a large computer projection screen centered at eye level and to the front of the subject. This was partitioned into four quarters with one task running in each section. The subject was required to move a track ball to the correct positions and press track ball buttons to register responses. Incorrect responses were noted with a computer beep and the subtask was reset. Correct responses also reset the subtask but with no audible beep.

Following the familiarization trial, the subject was given at least a 48-hour break before a data trail was initiated. For the actual testing, the tests described for the basic 15-minute epoch were repeated 16 times for a total of 4 hours of testing. A break was given at the 2-hour point of the 4-hour test. This lasted between 5 and 7 minutes. The subjects were allowed to dismount the testing apparatus, remove their helmets, visit the restroom, drink water, and rest in the remaining time. They remounted the MARS and were connected to the instrumentation. Testing was reinitiated for the remaining 2 hours. A break of at least 48 hours between data trials was scheduled to ensure recovery from fatigue.

Helmet loads

In determining the current recommended practice for helmet loading for U.S. Army aviation, the USAARL used short duration exposure not exceeding 20 minutes, and used 12 helmets. The USAARL determined that 90 N·cm was the limit for head-supported loads measured relative to the AO complex as determined from head pitch responses. That is, the head pitch response was greater for helmets with a torques larger than 90 N·cm as compared to lower torque helmets. The lower torque helmets were not different from the no-helmet case. Figure 4 shows these results with the higher helmet torques showing a greater head pitch response over both the lower torque helmets and the unloaded head.

For the current investigation, it was impractical to test each of the original 12 configurations for long-duration exposure. This would have required at least of 567 hours of testing, or more than one-half of a year of experimentation. Subject availability would have been severely limited for such an effort. Therefore, helmet configurations chosen for the current study were selected to cut diagonally across the helmet configurations shown in figure 5 with the highest load of 4 kg and a center of mass at +6 cm relative to the AO complex, to a helmet configuration of 0.5 kg with a center of mass at the AO complex.

The four helmet configurations are shown in figure 6. These also represent helmet loads seen in the Army aviation environment: the standard SPH-4B aviator helmet, an SPH-4B helmet with the sun visor down, an SPH-4B with the ANVIS NVG, and an SPH-4 with the ANVIS NVG and an M-43 chemical mask. The static weight moment of these helmets is given in table 1.

Subject grouping and helmet rotation

When subjects were selected for participation in this study, they were placed in four groups. Group 1 was filled with the first three. Similarly, the other groups were filled sequentially as subjects entered the protocol.

Helmet presentation was performed using a rotational paradigm. This was used rather than a random presentation to allow for the testing of presentation effects. For example, group 1 was presented with helmets 1, 2, 3, and then 4. For subsequent groups, the helmet presentation was rotated by one helmet with Group 2 being presented with helmets 2, 3, 4, and then 1. Table 2 shows the complete rotation for each group.

Table 1.
Helmet description with weight moments.

Helmet description	Measured weight moment (helmet alone) (N·cm)	Estimated weight moment (system) (N·cm)	Experimental weight moment (system) (N·cm)
SPH-4B	-19.5	103.4	122.9
SPH-4B with visor down	19.7	142.6	149.8
SPH-4B with NVG	144.6	267.5	280.2
SPH-4B with NVG and M-43 mask	297.8	420.7	410.8

Table 2.
Helmet configuration and subject grouping.

Group	Subjects	Helmet
1	1, 2, 3	1, 2, 3, 4
2	4, 5, 6	2, 3, 4, 1
3	7, 8, 9	3, 4, 1, 2
4	10, 11, 12	4, 1, 2, 3

Instrumentation

Position measurement system

The instrumentation discussed in this section applies only to the position measurement system. This limitation was imposed because the position data were the only ones analyzed in this report. Instrumentation and data analysis information pertaining to the other portions of the complete experiment are available at USAARL.

Positional recordings were performed using a Northern Digital Optotrack model 310 position measurement system. This uses three cameras that are triangulated to measure three dimensional positions of pulsed infrared diode markers. The resolution of the Optotrack system varies in relation to the recording distance between the cameras and the markers. For the current effort, resolutions were calculated to be less than 0.01 millimeters.

Thirteen active pulsed infrared markers were placed in the view of the three camera Optotrack system. Three markers were placed on the bite bar, three on the seat, three on the helmet, two on the sternum fixture, and two markers on the T1 fixture. Marker locations for the bite bar are shown in figure 7. Marker data were acquired at a rate of 200 frames per second, with each frame comprising the 13 markers. Raw sensor position data were stored on computer hard disk and later converted to actual positional measurements following testing.

Multiaxis ride simulator

The MARS is a three-axis (X, Y, Z) WBV platform capable of simulating helicopter motion. It can reproduce vibration frequencies ranging from 1 Hz to 35 Hz, ± 3 dB, with peak vibration spikes up to five times the force of gravity. Vibration data from a UH-60 helicopter were acquired by placing a triaxial accelerometer on the seat frame and recording accelerations while flying at a straight and level attitude at normal cruise speeds. These were then sampled by the MARS and reproduced to recreate the UH-60 vibration on the seat rail supporting the test UH-60 seat bolted to the top of the MARS. A complete description of the MARS can be found at appendix C.

Data analysis

Only the position data of the biomechanics test will be analyzed in this report. Because of the multidisciplinary nature of this effort, other data sets were distributed to qualified investigators for analysis. For example, the EMG data were offered to muscle physiologists, and cognitive performance data were offered to the research psychologists. Consolidated results from the various disciplines will be developed into a comprehensive report. The discussion of the data analysis procedures are limited to the position measurements of the head, head motions, and statistical analyses of these data.

Equations of motion

Position data from the bite bar were collected for each of the 16 epochs covering the 4-hour test. The raw Optotrack sensor data were converted to three dimensional position data following testing. These were processed to create head motion data for the midsagittal plane covering head pitch, X, and Z displacements. These investigations were limited to planar motion because the head was shown to move only in a planar fashion due to axial vibration (Butler, 1992; Paddan and Griffin, 1988). UH-60 vibration data are primarily axial with only 10 percent of the signal found in the other primary directions.

The purpose of the equations of motion for the head (derived below) was to determine from the sampled bite bar data the motions of the head at the AO complex. This was chosen as the point of interest for head motion because it is the location of the pivot point of the head on top of the spine. The muscles in the neck supporting the head act through this point. The equations of motion were derived from the geometry of the head relative to the AO complex and the bite bar markers. Figure 7 shows the bite bar markers and the AO complex superimposed on a fictional profile of a subject's head and neck. Lateral photographs of the subjects were taken to capture the position of the bite bar relative to anatomical landmarks. The points (X_1, Z_1) and (X_2, Z_2) represent the most anterior and inferior markers on the bite bar, respectively (figure 8). Given three dimensional positional measurements of (X_1, Z_1) and (X_2, Z_2) , the Z-axis, X-axis, and pitch motion at the AO complex, or at the point (X_3, Z_3) , can be determined as follows.

First, AO complex pitch motion, θ_1 , can be found using positional measurements directly from the bite bar, yielding

$$\tan \theta_1 = (Z_1 - Z_2) / (X_2 - X_1) \quad (1)$$

Next, the X and Z displacements of the AO complex can be found using

$$X_3 = X_1 + (d_1 + d_3 + d_4) \cos \theta_1 + (d_2 - d_5 + d_6) \sin \theta_1$$

$$Z_3 = Z_1 + (d_2 - d_5 + d_6) \cos \theta_1 + (d_1 + d_3 + d_4) \sin \theta_1$$

where d_1 is the distance measured inferior from the bite bar to a perpendicular from the external auditory meatus (EAM), and d_2 is the length of the perpendicular to the EAM (see figure 9). The variables d_3 through d_6 can be redefined as follows

$$d_3 = d_7 \sin \theta_2$$

$$d_4 = d_8 \cos \theta_2$$

$$d_5 = d_7 \cos \theta_2$$

$$d_6 = d_8 \sin \theta_2$$

where $d_7 = 22$ mm and $d_8 = 10$ mm from physical measurements (... ref 20...), and where θ_2 is measured from lateral photographs capturing the subject's profile. Substituting the values of d_7 and d_8 in the above equations, the X and Z coordinates of the AOC (in millimeters) may be expressed as

$$X_3 = X_1 + (d_1 + 22 \sin \theta_2 + 10 \cos \theta_2) \cos \theta_1 + (d_2 - 22 \cos \theta_2 + 10 \sin \theta_2) \sin \theta_1 \quad (2)$$

$$Z_3 = Z_1 + (d_2 - 22 \cos \theta_2 + 10 \sin \theta_2) \cos \theta_1 - (d_1 + 22 \cos \theta_2 + 10 \sin \theta_2) \sin \theta_1 \quad (3)$$

Signal processing of head motion

The equations of motion (1, 2, and 3 above) were used to determine head kinematics at the AO complex. The head motion data of this experiment characteristically are vibration data. This type of information is analyzed routinely in the frequency domain using a Fourier analysis technique. The emphasis in Fourier analysis is to detect peak resonant responses and resonant frequencies. Care must be exercised in applying the Fourier techniques, especially the discrete Fourier transform (DFT), to avoid inadvertently contaminating the results. Therefore, head motion data were processed to capture peak resonant responses using standard signal processing techniques.

The signal processing techniques used in analyzing head motion data began with extracting a 256 point segment from the 1500 point data sequence generated for each head motion at each of the 16 epochs. This small sequence was first filtered to remove any average (DC) value. Removing the DC value eliminated any large constant signal that would have contaminated low frequency responses. Because head pitch resonance is at a low frequency of 4.5 Hz, this step was necessary to ensure good fidelity.

The extracted signal was multiplied by a Hamming window (Harris, 1978). This process, known as windowing, is used to remove any discontinuities at the ends of the signal. This step is required due to an assumption in DFT analysis that the extracted signal is representative of the larger complete signal. In fact, the mathematics of the DFT require that the extracted signal can be concatenated to itself to create a longer sequence. In this concatenation procedure, there can be no discontinuities when the end of one signal section is attached to the beginning of the repeated signal section. If discontinuities are not removed, the resultant DFT will be contaminated with high frequency signals posing as low frequency data.

Another assumption for applying the DFT is that the analyzed signal must meet the condition of wide sense stationarity. This means that the signal does not have a changing mean or standard deviation. It would appear that a rejection of the null hypothesis (H_0 : that there would be no change in head motion over time) would be a violation of this criterion. However, if the time segment for which the analysis is performed is short enough, then wide sense stationarity can be assumed to have been satisfied.

The windowed data were processed using a high speed DFT routine (Digital Signal Processing Committee, 1979) originally written in FORTRAN and translated into C for this report. Subsequent 256 point data segments were similarly processed using an overlap and add method (Richards, 1976). This technique further increased the fidelity of the DFT results. Finally, resonant peaks were identified and extracted for later statistical analysis. A complete flow of signal processing techniques is shown in figure 10.

Statistical analysis

Head motion data analysis began by viewing frequency domain plots. These were used to verify the quality of the data. Expected results included the identification of four peaks of decreasing size ranging from 4.25 Hz to 17 Hz. The first peak, at 4.25 Hz, was expected to be the largest peak, representing the resonant head motion response generated from the one blade passing frequency of the UH-60 main rotor blade system. The one blade passing frequency is the frequency at which one main rotor blade completes one revolution. The next peak was expected at around 8.5 Hz representing the two blade passing frequency of the UH-60 and the first resonance of head motion. The third peak occurred around 12.75 Hz representing the second resonant peak of head motion. The last peak, at around 17 Hz, represented the four blade passing frequency of the UH-60, as well as the fourth resonance of head motion and the second resonance of the two blade passing frequency.

Peak primary resonant head motion data were found for head pitch, X and Z motion using a local maximum search routine centered at 4.5 Hz. Data were arranged to perform two way analysis of variance (ANOVA) using helmet and epoch as the independent variables. Where significant differences were found, a Tukey multiple comparison of means test was performed within independent variables to identify differences.

Assumptions

The following assumptions were made in support of this study:

- a. The volunteer aviators for this study were a representative sample of the Army aviator population.
- b. The MARS WBV simulator created the same biomechanical stress in the aviators as actual UH-60 helicopter flights.
- c. Applying myoelectric sensors and position sensors to the volunteer aviators did not alter their biomechanical response as compared to the noninstrumentation situation found in actual UH-60 helicopter flight.
- d. The motion of the head on the neck due to UH-60 WBV exposure was of the range and rate requiring only static voluntary muscular contraction to support the head.
- e. Subject posture did not change throughout the 4-hour test.
- f. The motion of the head and neck resulting from UH-60 WBV was limited to the midsagittal plane with pitch motion dominant over X and Z translation.

g. Aviators spend 80 percent or more of their time in the crew station in an upright posture, reflecting the appropriateness of the upright posture selected for the experimental trials.

Analysis

The head motion data acquired in this study were generated from a vibrating platform simulating WBV experienced by UH-60 helicopter pilots. Because vibration data are best described in terms of their magnitude and frequency, the calculated time domain head motion data were processed to generate frequency domain data. The initial frequency domain analysis was performed to assess the quality of the frequency domain data resulting from the application of the signal processing routines.

An example of the frequency domain data is shown at figure 11. The plot was generated from one subject, one helmet, using the first epoch of the 16 epoch test. It shows the dominant head pitch resonance at 5.1 Hz with a magnitude of 0.055 degrees. Other peaks occurred at frequencies of 8.6 Hz, 12.9 Hz, and 17.2 Hz. These upper three peaks correspond to the resonant characteristics of the UH-60 main rotor blade frequencies. For example, the one blade passing frequency of the UH-60 is at 4.3 Hz. Harmonics of this frequency are at 8.6 Hz for the two blade passing frequency, 12.9 Hz for the three blade passing frequency, and 17.2 Hz for the four blade passing frequency.

Examples of X and Z motion are shown in figures 12 and 13. Both plots show the head resonance at 5.1 Hz. The other three expected peaks at 8.6 Hz, 12.9 Hz, and 17.2 Hz are evident to varying degrees in the plots. The X motion data of figure 12 show a small peak at 8.6 Hz, with the other peaks evident only when viewing the supporting data. The Z motion data of figure 13 show the 8.6 Hz peak along with the 12.9 Hz peak. The peak at 17.2 Hz is only evident from the supporting data. By yielding expected magnitudes and frequencies for head pitch, figures 11, 12, and 13 serve to confirm the functioning of the Fourier analysis routines, and confirm the calculations of head pitch motion.

The purpose of generating the frequency domain data was to capture the peak head pitch, X, and Z motion data occurring at resonance during each time period. Head motion data were processed as described above to generate frequency domain data for each of the 16 epochs covering the 4-hour data runs. An example of the head pitch motion for each of the 16 epochs is shown in figure 14 for one subject and one helmet. The resonant peaks at 5.2 Hz range from 0.029 degrees to 0.575 degrees, a range over four times that of the other peaks.

The variability in the resonant peak shown in figure 14 was investigated to assess the effect of helmet type or exposure duration on peak amplitude. This analysis was performed for each head motion. A local maximum was found using a peak picking algorithm to capture the peak data ranging from 3 Hz to 8 Hz. Figures 15-18 show, for each helmet, peak head pitch data for

each of the 12 subjects plotted by epoch. The X and Z head motion examples are similar, but for brevity, are not shown.

The peak response versus epoch data of figures 15-18 show relatively flat responses for head pitch over time with occasional outliers. There appears to be no apparent pattern regarding the outlier data relative to timing, subject, or helmet. These data were averaged for all subjects and plotted in figures 19-21. These averaged plots show head motion for each of the four helmets plotted by epoch.

The pitch data of figure 20 are relatively flat, and may even be decreasing over time for each helmet. This figure also shows an increasing pitch magnitude for helmets 2 through 4, that is, for helmets of increasing torque loads. This trend appeared only in the first half of the test period. In the second half, the separation in the pitch response among the three highest torque helmets appeared to taper off over time. The lowest torque load, helmet 1, did not follow this hierarchical trend in the first half of the testing, remaining with a pitch response that is larger than the next higher torque helmet. Near the end of the testing, the lowest torque helmet had the least pitch magnitude response.

Head X motion and Z motion of figures 20 and 21 appeared similarly flat over time. The only trend that was remotely apparent was for an increased magnitude response for X and Z motion with the lowest torque helmet (helmet 1) as compared to the heavier torque helmet (helmet 4). Average X motion response also remained approximately 50 percent of the Z motion response.

Statistical analysis

Statistical analysis was performed to assess the significance of the trends shown in the above plots. A two way ANOVA was performed using independent variables of epoch and helmet. The purpose of this was to assess the effects of either time, or helmet torque, or the interaction between these two variables, as having an effect on the peak head motion. Results indicated significant differences ($P < 0.05$) for helmet torque, but no significant differences for epoch, and no significant interaction effects. These results require that the first null hypothesis for exposure duration not be rejected. That is, the hypothesis that head motion will not change as a result of exposure duration is not rejected. However, the second null hypothesis—that head motion will not change as a result of helmet torque—is rejected. Written in the alternative format, and for the conditions of this test, helmet torque does have an effect on head motion, but exposure duration does not.

Even though ANOVA results indicated no significant differences for epoch, or exposure duration, a multiple comparison of means test was performed for helmet type at each epoch. A variety of tests that are designed to protect the user from violating basic statistical assumptions are available to perform multiple comparisons of data sets. For example, when using contrasts with ANOVA, it is assumed that one sample group will be used in a comparison only one time.

If it is compared more than once, a correction—called a Bonferroni correction—must be applied. This correction divides the level of significance by the number of comparisons being made. The Tukey test is a procedure with a built-in correction factor.

Table 3.
Tukey test for helmet at each epoch.

Motion	Epoch	Differences ($p < 0.05$)
Pitch	0	2≠3,4
	1	2≠4
	2	2≠4
	6	2≠4
X	0	1≠4
Z	3	1,2≠4

The Tukey test was used to produce the results of table 3. The data of table 3 indicate that differences exist among helmets in the early epochs but not in the later epochs. Consistent differences were found between helmets two and four, that is, the highest torque helmet was different from the next-to-lowest torque helmet. Only one epoch resulted in differences for X or Z motion. Here, consistent differences were found between helmets one and four—the highest and lowest torque helmets.

The ANOVA results were used to justify averaging across epoch and performing a multiple comparison of means for helmet type. The Tukey test was performed for helmet torque, resulting in significant differences as shown in table 4. These data indicate that the highest torque helmet is significantly different from the two lowest torque helmets, and the next-to-highest torque helmet is significantly different from the lowest torque helmet, for all head motions. Figures 22-24 show the averaged head motion data (for epoch and subject) for each of the four helmets by head motion.

Table 4.
Tukey test for helmets.

Motion	Differences ($p < 0.05$)
Pitch	1,2 \neq 3,4 3 \neq 4
X	1 \neq 2,3,4 2 \neq 3,4
Z	1 \neq 3,4 2,3 \neq 4

Discussion

The two primary results of this study are that: (1) head motions were affected by helmet torque, and (2) head motions did not change with exposure duration. The first result confirmed the findings of earlier studies showing that head pitch response increased when helmet torque increased. The second result was unexpected. It was expected that head pitch response would increase over time with the onset of muscle fatigue. This fatigue would cause a reduction in the spring constant of the muscle and a resultant shift in head pitch resonant response to lower frequencies. This shift would pass the head pitch response through the UH-60 one-blade-passing resonant frequency, which is close to, and lower than, the head pitch resonant frequency. When the head pitch resonance frequency hit the UH-60 resonance frequency, there would be an increase in the input vibration with a resulting increase in head pitch response. That there was no increase in head pitch response suggests that this mechanism was not active under the conditions of this study. The details supporting this conclusion will be discussed along with the signal processing details behind the data analysis.

One error commonly made in signal processing is that researchers string together analysis routines without knowing the effects of each of the steps on the quality of the results. Simply stringing routines together without knowing and testing for the relative effects of each stage of the algorithm can lead to erroneous results. For example, decisions must be made as to the time domain window length, the window shape, the sampling frequency, the amount of overlap used, the effects of filtering, and other factors that affect the overall quality of the frequency domain results. The algorithm used for this study was developed to yield low frequency data that could be used to distinguish between spikes that were separated by less than 1 or 2 Hz.

The frequency response plots of figures 11-14 are examples of the results of the signal processing routines outlined in figure 10. The original data contained large low frequency spikes that were filtered out using a high pass frequency domain filter. These were most likely due to small fluctuations in posture arising from breathing, beating of the heart, and other autonomic

postural changes. Although such phenomenon may be of interest to other investigators, they have little effect on head pitch dynamics and are not of interest to the current study. The spikes were located at a frequency below the 5 Hz head pitch response and were separated from the head pitch resonance by a distinct minimum in the data. This minimum, typically located around 3 to 4 Hz, was used as the cutoff frequency for the high pass filter.

Even though these low frequency spikes were large—as much as 10 times the size of the head pitch resonant spike—the signal processing routines were designed to be robust enough to separate them from the resonant head pitch spikes. The difficulty here is that often times a large spike can spread over into adjacent frequencies and cover up data spikes that are close to the center frequency of the adjacent spike. Occasionally, another small spike was detected at around 4.3 Hz that looks like a low frequency shoulder on the head pitch resonant spike. This shoulder actually was due to the one-blade-passing-frequency of the UH-60, and is the primary resonant peak of this helicopter. The other small spikes in the frequency domain plots, those beyond the head pitch resonant peak, are harmonics of this 4.5 Hz spike.

The UH-60 resonant peak is of interest in its relationship to the head pitch resonant peak and the effects of muscle fatigue. One possible result of muscle fatigue could be a reduction in head pitch resonant frequency through the UH-60 resonant peak. A possible explanation for this shift could be a reduction in muscular tension in the neck. This could decrease through a reduction in the number of muscle fibers firing in the active motor units, by an overall reduction in the firing motor unit pool, by recruiting new motor units that have less of a capacity to produce tension, or by any combination of these mechanisms. A reduction in tension would be represented in biomechanical modeling by a reduction in the spring constants of a mass-spring system where the spring represents the muscle. This would result in a reduction in the resonant frequency of the system. For example, hang a mass off a spring and it will bounce up and down at a particular frequency. If the spring is replaced with a weaker spring, the mass will bounce up and down at a slower frequency.

A gradual reduction in the head pitch resonance would have moved the resonant frequency through the 4.3 Hz UH-60 resonant frequency. At this frequency there would have been an increase in the amount of energy exciting the head-neck system. Under these conditions, head pitch should increase. However, in this study, head pitch was shown to remain flat over time, or may even have shown a decreasing trend. One possible explanation for this is that muscle fatigue did not occur, at least to the extent that there was a reduction in muscle tension. Another explanation is that fatigue did occur, but the inherent mechanisms of maintaining muscle tension were enough to maintain head pitch control. The head pitch data analyzed in this report were not sensitive enough to indicate muscle fatigue. The data captured in the other phases of the overall experiment, however, may be useful in assessing the degree of muscle fatigue.

Head pitch still could be used to assess changes in resonant responses, and could indicate changes in muscle function. For example, if a random vibration replaced the UH-60 vibration for a brief period in the biomechanics test, head pitch resonant frequency could be tracked more

accurately over the period of the entire test. Or a transfer function, showing the degree of output response resulting from the input function, could be used with the existing data to assess changes in resonant characteristics. These tests could be performed with the existing data and may offer other interesting insights into the nature of the head pitch response.

The plots of figures 15-18, showing head pitch response for each helmet and for all subjects over time, contain occasional large spikes in the data sets. These should not be interpreted as significant data trends as there appears to be no regularity or pattern to their occurrence. For example, no trends are apparent relative to the epoch, subject, or helmet. These spikes probably should be interpreted as outliers in the data sets. Nevertheless, they did have an effect on the statistical analysis for at least one test, showing an increase in variance where they occurred among the epochs. This caused the rejection of a statistical result for Z head motion over time for a test requiring uniformity of variance. However, for the most part, these outliers were not factors in the overall statistical analysis.

The averaged plots of figures 19-21 reinforce the nearly flat head motion response seen in the earlier plots for pitch, X and Z motion across epochs. However, differences do exist in the relative response for head pitch among helmets in the first half of the experiment that do not appear in the second half. For head pitch motion, significant differences were found among the helmets in the first three epochs, and in the sixth epoch. Only the third epoch showed significant differences for Z motion, and only the zeroth epoch showed differences for X motion.

The plot of figure 19 shows a trend for decreasing pitch response with decreasing helmet torque. This trend fits for helmets 4, 3, and 2, but not for helmet 1. Helmet 1 shows an increase in head pitch response over that of the next two higher torque helmets. The data of table 1 offers an explanation. Helmet 1 was configured with a torque that actually decreased the net torque about the AO complex. The torque for the head alone was measured at 122.9 N·cm. Helmet 1 had a center of mass that was behind the AO complex and caused a reduction of the total system torque (the combined head and helmet torque). The system torque was estimated at 103.4 N·cm, or 19.5 N·cm less than the head alone. The net effect of this reduction in torque is thought to have caused an instability in the head-neck system resulting in an increase in head pitch response.

Two way ANOVA for helmet type and epoch showed significant differences for helmet type, but no differences for exposure duration. This latter result was unexpected. The expected result was an increase in head pitch motion coincident with the onset of muscle fatigue. Muscle fatigue was expected certainly with helmet 4, likely with helmet 3, and potentially with helmets 2 and 1. The duration of the test alone was expected to induce posterior neck muscle fatigue and affect head pitch motion. Subjects often reported fatigued necks at the end of the testing. Most subjects would stretch their neck muscles through multiple range of motion movements apparently to remove any stiffness resulting from the testing. However, the results of this test contradict the expected result. No effect of exposure duration was evident. These results suggest that aviators can maintain head pitch control independent of helmet torque for up to 4 hours of exposure under the conditions set by this study.

The lack of exposure duration effects allowed the pooling of the data across epoch and a subsequent multiple comparison of means test for helmet type. This showed differences among the helmets that were similar to those reported in earlier short-duration head-supported mass studies performed by the USAARL. For head pitch response, the highest torque helmet, helmet 4, was shown to be significantly different from the two lowest torque helmets, helmets 1 and 2, but not different from helmet 3. Helmet 3, the next highest torque helmet, also was found to be different from the two lowest torque helmets. Similar trends were seen for both X and Z head motion with helmet 4 being significantly different from helmet 1. Other differences existed as shown in table 4. This result supports the recommended practice of limiting the helmet torque to 90 N·cm measured relative to the AO complex.

Head pitch response generally increased going from helmet 2 through helmet 4. This trend, however, was broken by helmet 1, which showed a pitch response averaging between the responses of helmet 2 and helmet 3. A possible explanation of this could be that helmets 2 through 4 added to the torque of the combined head-helmet system. This is the load controlled by the muscles in the neck. The added torque increased the apparent load of a mass-spring system resulting in an increase in resonant motion magnitude with an increase in helmet torque. However, helmet 1, the lowest torque helmet, actually unloaded the head-neck system. This is possible if the helmet added a negative torque measured relative to the AO complex, even though there was an overall increase in added mass. This could result in a combined head-helmet torque that was actually less than the torque created by the head alone, a torque normally controlled by the muscles of the neck. By unloading the head-neck system, the control of head pitch may become erratic resulting in an increase in resonant pitch response.

The X and Z head motion showed a decreasing response for increasing head-supported loads, as shown in figures 23 and 24. This can be explained by recalling that head motion was calculated at the AO complex. Here, the added mass was modeled as a point mass on top of the spine. By adding mass to the system, the momentum of the overall head-neck system was increased. This resulted in a dampened X and Z motion with increased head-supported mass. The rest break at the 2-hour mark in the 4-hour test is similar to the rest break aviators experience in long-duration flights when they must land and refuel. During this rest break, the subjects were allowed to remove the helmet and dismount the test platform for a period of less than 10 minutes. This time was thought to be long enough to experience recovery of mild muscle fatigue, and prepare the subject for the remaining 2-hour test period. Though the traces of figures 19-21 were relatively flat for head motions over time, differences did occur among the helmets in the first half of the test, compared with no differences found in the second half. Recovery here would have been indicated by a restoration of these differences among the helmets. Thus, there appeared to be a continuation in the trends of head motion response as contrasted to any recovery effects of the rest break. If muscle fatigue occurred, that discovery will be the subject of other parts of the overall experimental protocol.

Conclusions

The results of this study investigating the effects of head-supported mass under long-duration WBV exposure indicated there was no effect of exposure duration on head pitch, X or Z motion calculated relative to the AO complex for helmets ranging up to 90 N·cm for exposure durations of up to 4 hours. However, this study did show significant differences for helmet torque as measured relative to the AO complex, verifying the results of earlier short-duration studies of head-supported mass.

Recommendations

The practice of limiting the head-supported mass to 90 N·cm should be maintained. Future helmet designs should limit the added torque as measured in the gravity field and measured relative to the AO complex to 90 N·cm. Future studies of the effects of long-duration exposure to head-supported mass should be directed towards the investigation of muscle fatigue. These biomechanical investigations, coupled with investigations of psychophysical and cognitive performance, can produce a head-supported mass recommended practice that is robust enough to withstand the uncertainties of future aviator crew station requirements.

References

- Anthropometry and mass distribution for human analogues. Volume. I: Military male aviators. 1988. Fort Rucker, AL: US Army Aeromedical Research Laboratory. USAARL Report 88-05. March.
- Beer, Ferdinand P., and Johnson, E. Russell, Jr. 1988. Vector mechanics for engineers: Statics. New York: McGraw-Hill Book Company. 5th edition.
- Butler, Barclay P. 1992. Helmeted head and neck dynamics under whole-body vibration. Ann Arbor, MI: University of Michigan. Ph.D. dissertation.
- Butler, Barclay P., Lantz, Susan, and Alem, Nabih M. 1991. Measurement and analysis of neck muscle myoelectric activity, performance, and head and neck motion for varying head-supported weight moments in a simulated helicopter environment. Fort Rucker, AL: U. S. Army Aeromedical Research Laboratory. Research Protocol.
- Chaffin, Don B., and Anderson, Gunnar B. J. 1984. Occupational biomechanics. New York: Wiley and Sons.
- Digital Signal Processing Committee. 1979. Programs for digital signal processing. New York: IEEE Press. 1.2-7.
- Griffin, M. J. 1975. Vertical vibration of seated subjects: Effects of posture, vibration levels, and frequency. Aviation space and environmental medicine. 46:269.
- Guignard, John C., and Irving, A. 1960. Effects of low-frequency vibration on man. Engineering. 190:364.
- Harris, Fredric J. 1978. On the use of windows for harmonic analysis with the discrete Fourier transform. Proceedings of the institute of electrical and electronic engineers. 66:83.
- Matthews, P. B. C. 1972. Muscle spindles and their motor control. Physiological review. 44:224.
- McGill, David J., and King, Wilton W. 1989. Engineering mechanics, an introduction to dynamics. Boston: PWS-KENT Publishing Company. 2nd edition.
- Paddan, G. S., and Griffin, M. J. 1988. The transmission of translational vibration to the head. Journal of Biomechanics. 21:195,197.
- Richards, Paul I. 1976. Computing reliable power spectra. IEEE Spectrum. 3:90.

References (continued)

Sandover, J. 1978. Modeling human response to vibration, Aviation, space and environmental medicine: Biodynamics symposium. 339.

Sobotta, Johannes. 1990. Atlas of human anatomy. Baltimore: Urban and Schwarzenberg.
Jochen Staubesand, ed. Vol. 1.

Wilder, David. G., Woodworth, B. B., Frymoyer, J. W., and Pope, M. H. 1982. Vibration and the human spine. Spine. 7:254.

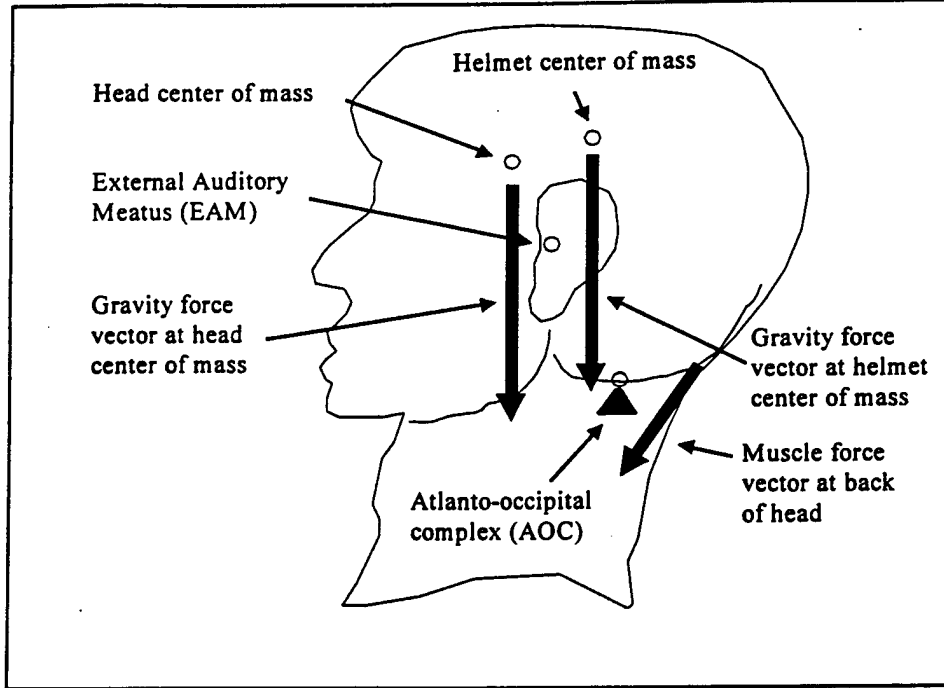


Figure 1. Force vectors. Profile of the head and neck showing the AO complex, head center of mass, helmet center of mass, and force vectors representing the gravity field and the posterior of the neck.

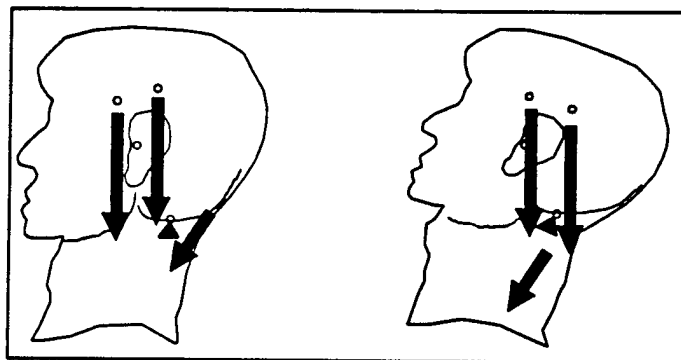


Figure 2. Force vector rotation. Profile of the head and neck showing the effect of rotating the face upwards and repositioning of the force vectors in the gravity field transfer to the head and neck.

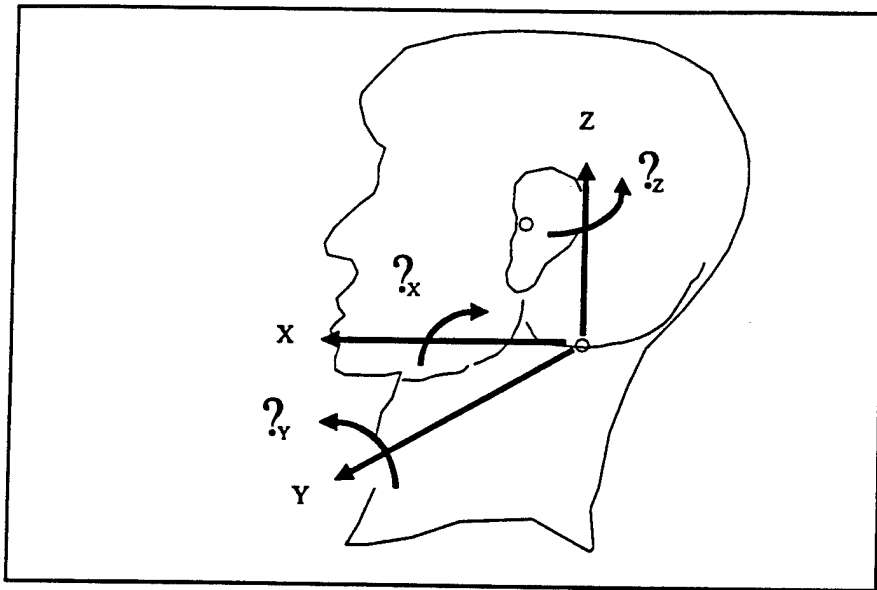


Figure 3. Head frame of reference. Coordinate axes with X, Y, and Z as the translational axes, and O_x , O_y , and O_z as the rotational axes.

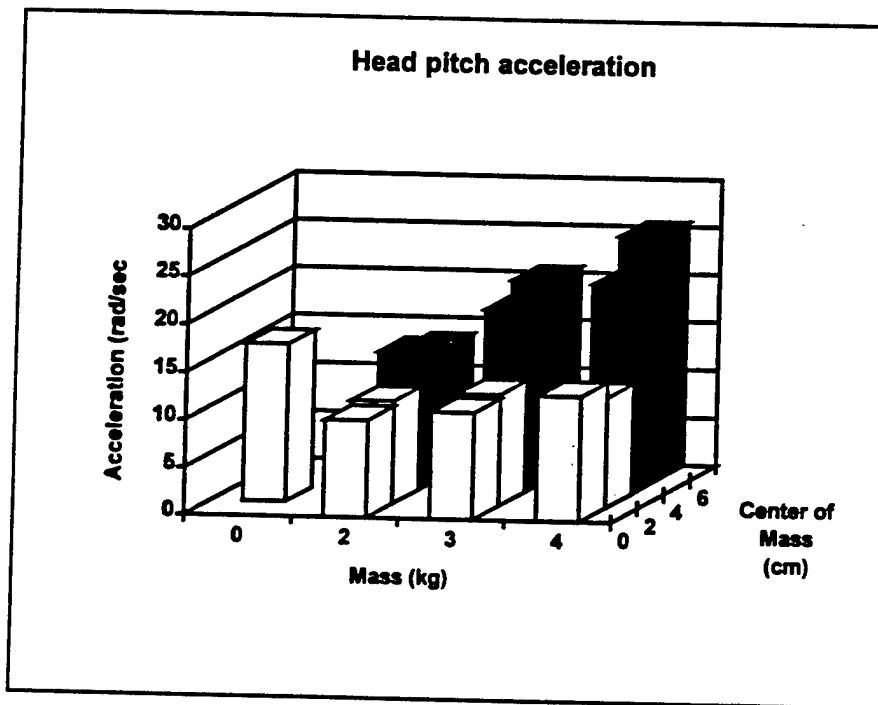


Figure 4. Short-duration head pitch response. Head pitch response for short-duration whole-body vibration exposure.

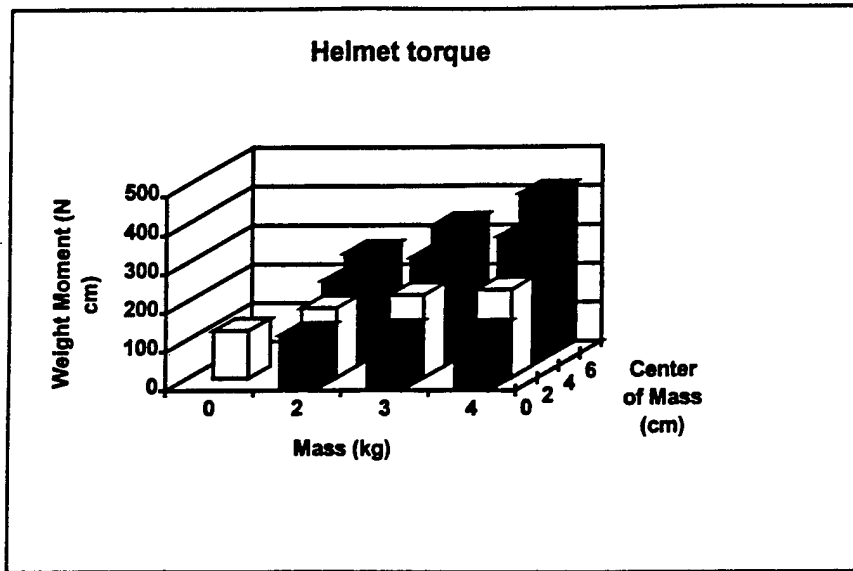


Figure 5. Short-duration helmet torque. Helmet torque for short-duration whole-body vibration exposure. Helmet torques represent system totals including the 122.9 N·cm of the head.

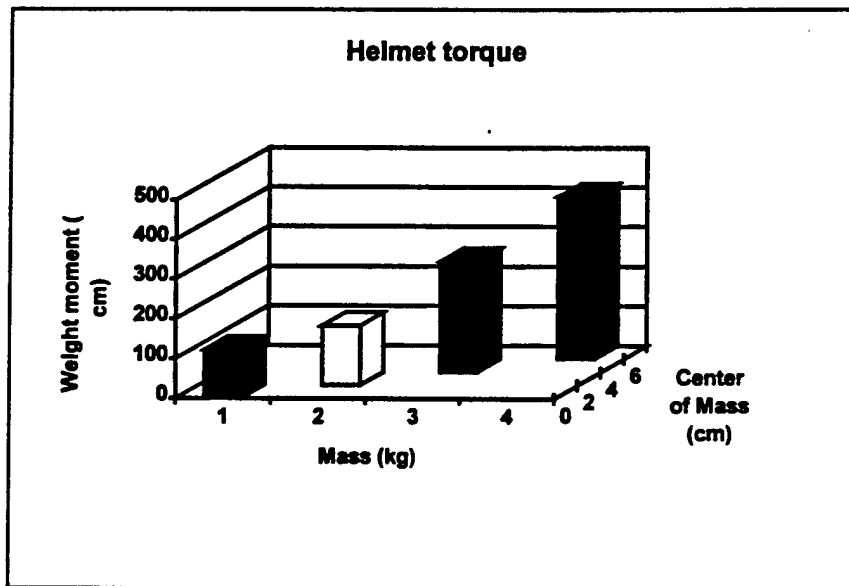


Figure 6. Long-duration helmet torque. Helmet torque for long-duration whole-body vibration exposure. Helmet torques represent system totals including the 122.9 N·cm of the head.

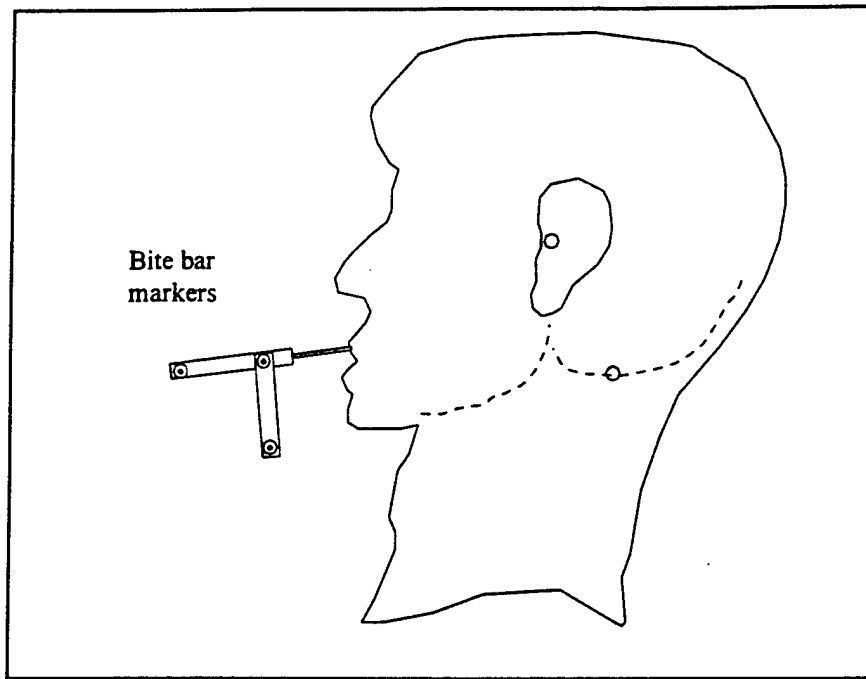


Figure 7. Marker location for the bite bar.

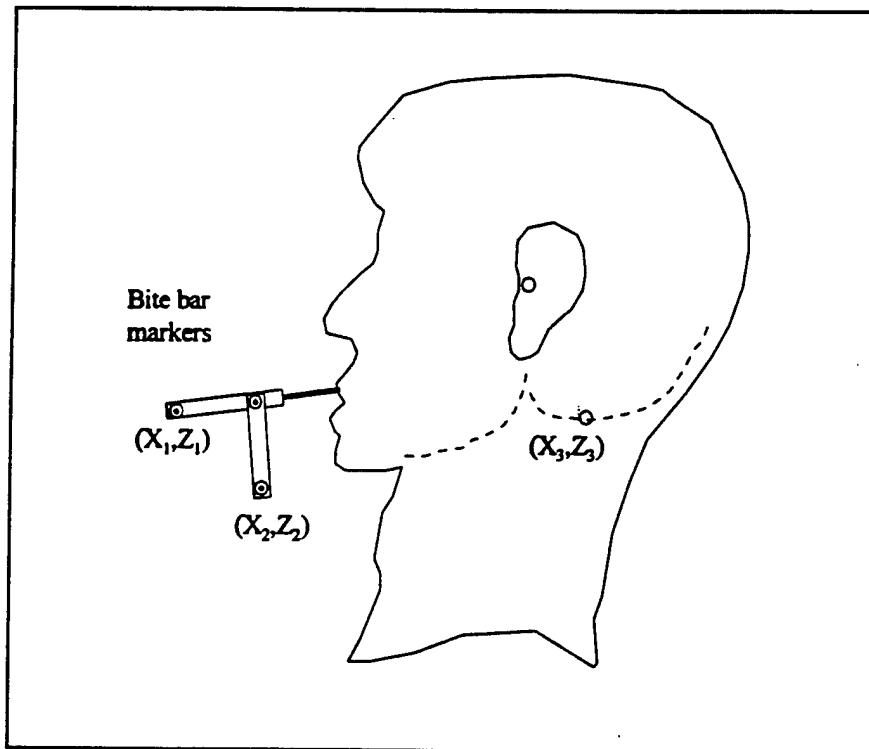


Figure 8. Bite bar coordinates.

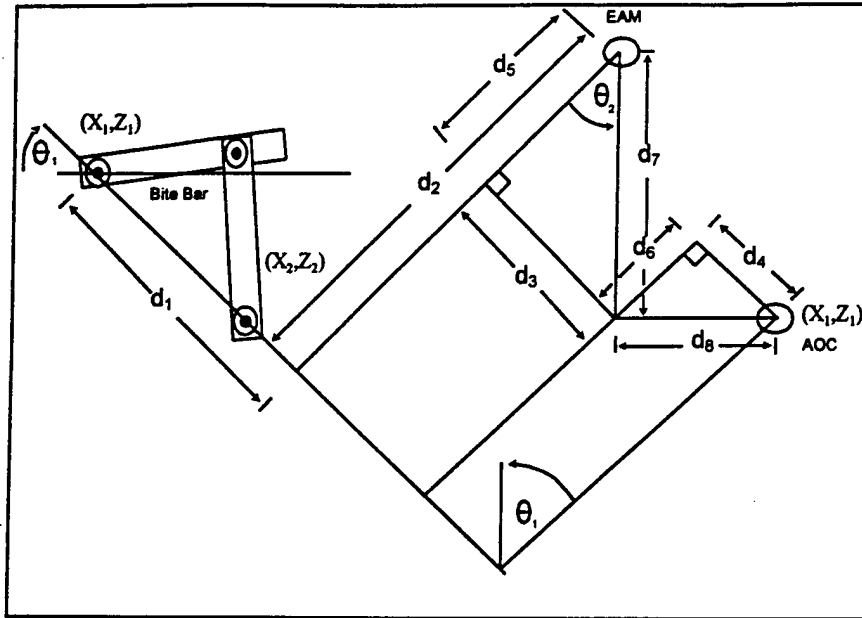


Figure 9. Bite bar geometry. The geometry of the bite bar and its relationship to the AO complex.

1. Generate AO pitch, X, Z motion
2. Data set size:
 - a. 1500 points /epoch
 - b. 16 epochs
 - c. 4 helmets
 - d. 12 subjects
3. 256 point time domain window
 - a. Overlap and average
 - b. Use 64 point shift
 - c. 5 shifts
4. Subtract off average
5. Hamming window
6. Subtract off average
7. FFT routine, radix 8
8. Average FFT results
9. Locate peak response
10. Locate frequency at peak response
11. Perform statistical analysis

Figure 10. Signal analysis flow chart.

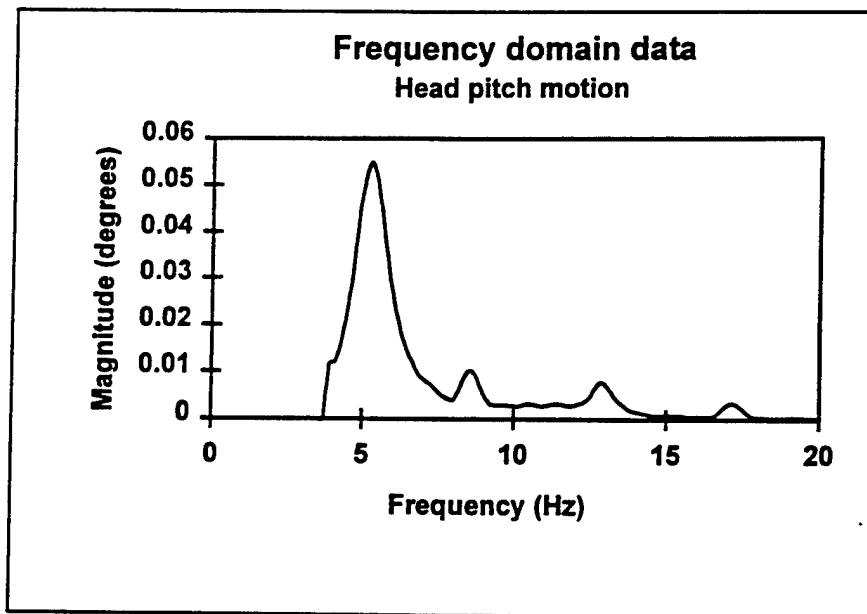


Figure 11. Head pitch motion. Frequency domain data for head pitch motion, subject 1, helmet 4, epoch 7.

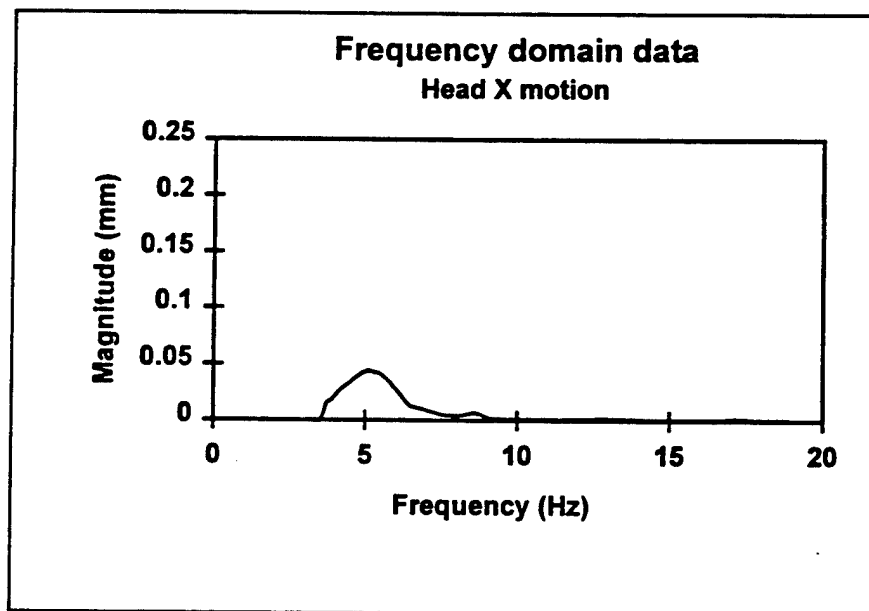


Figure 12. Head X motion. Frequency domain data for head X motion, subject 1, helmet 4, epoch 7.

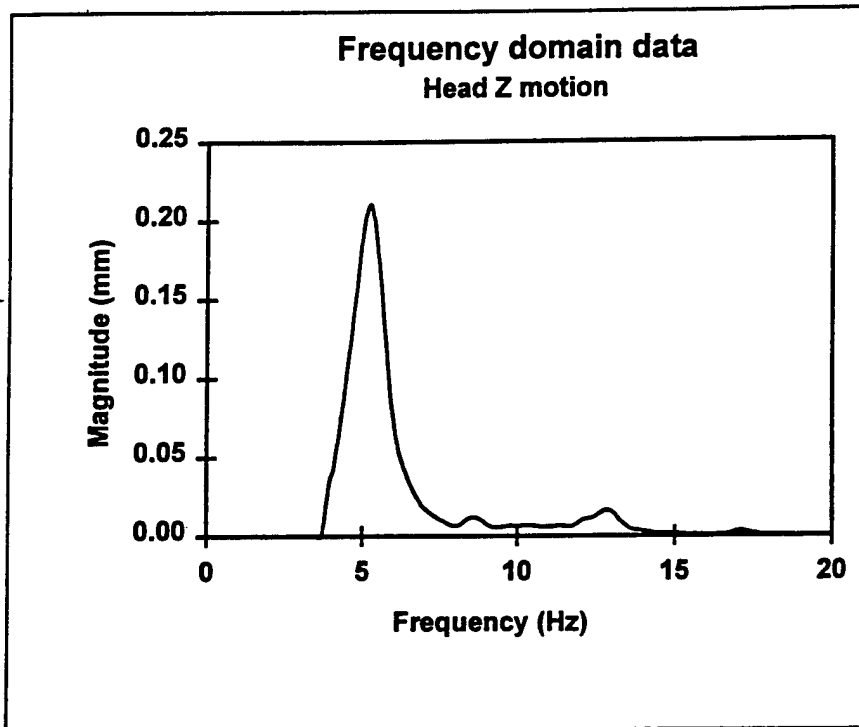


Figure 13. Head Z motion. Frequency domain data for head X motion, subject 1, helmet 4, epoch 7.

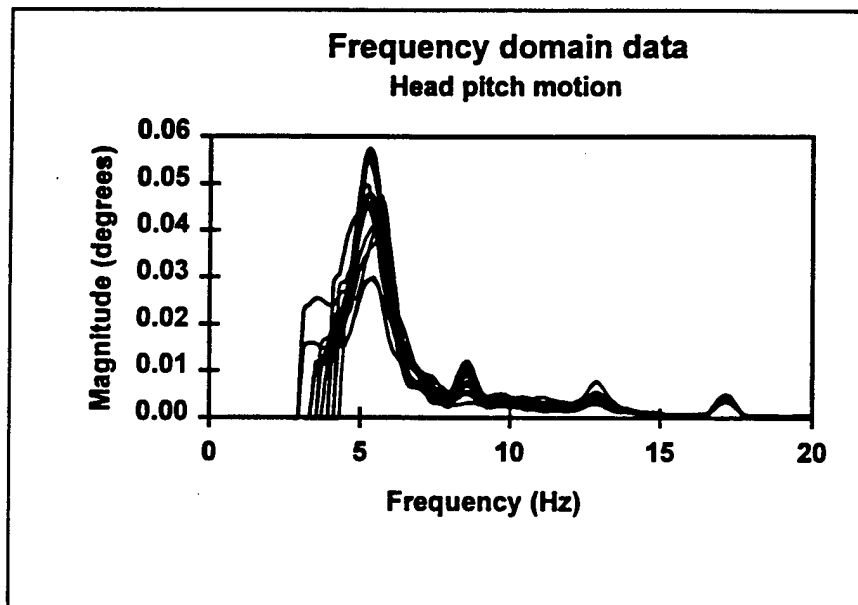


Figure 14. Head pitch peaks for 16 epochs. Frequency domain data for head pitch motion, subject 1, helmet 4, 16 epochs.

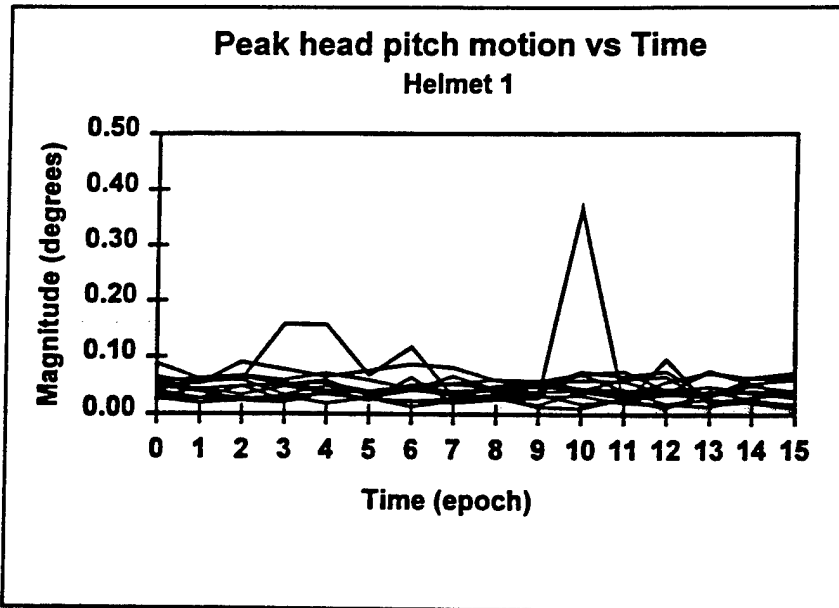


Figure 15. Peak head pitch versus time, helmet 1. Peak head pitch motion for each epoch, helmet 1, 12 subjects.

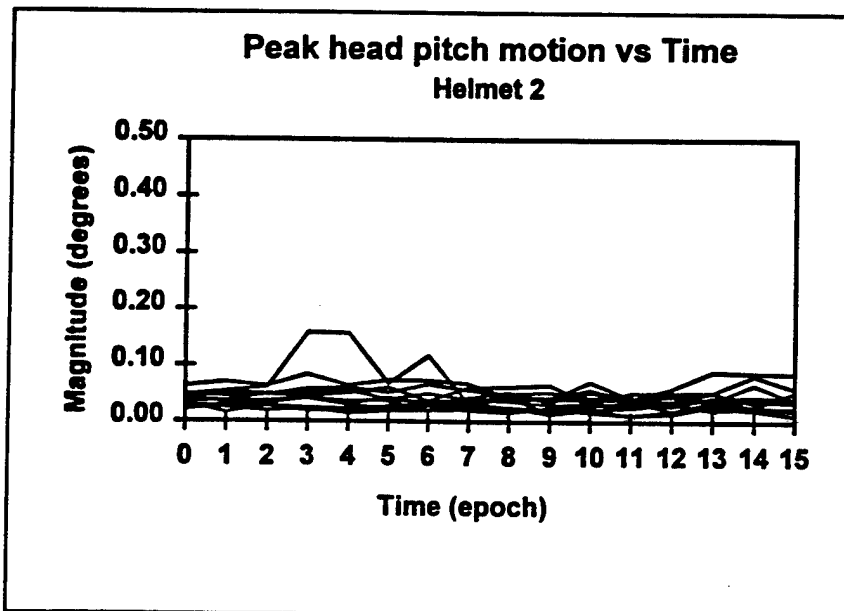


Figure 16. Peak head pitch versus time, helmet 2. Peak head pitch motion for each epoch, helmet 2, 12 subjects.

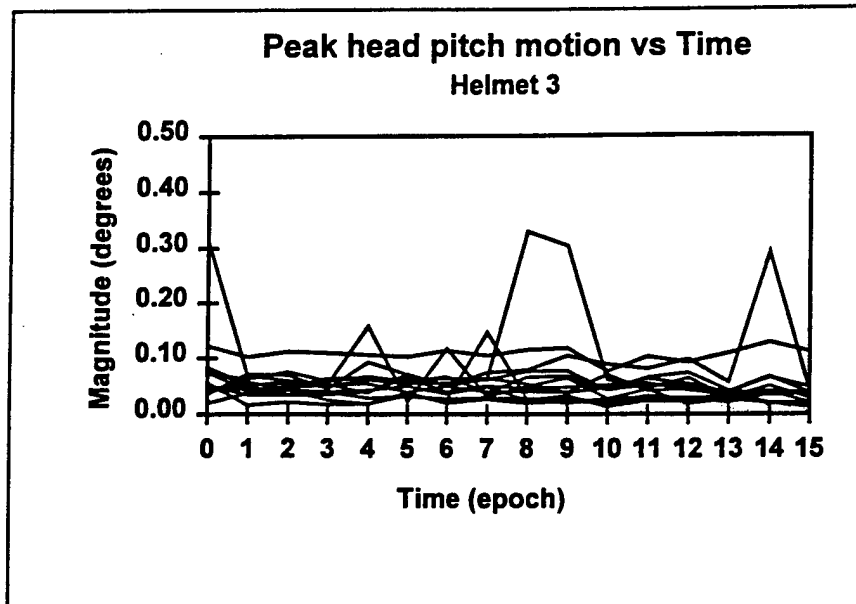


Figure 17. Peak head pitch versus time, helmet 3. Peak head pitch motion for each epoch, helmet 3, 12 subjects.

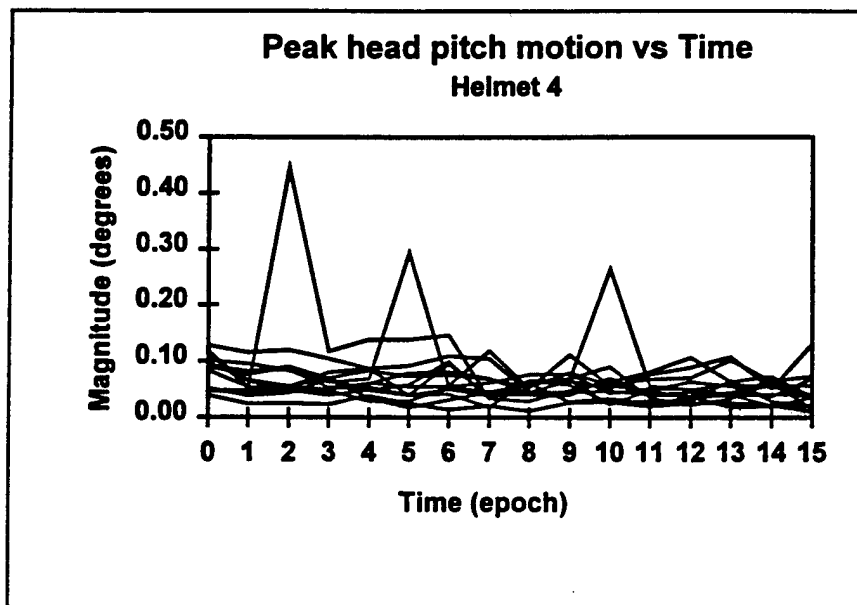


Figure 18. Peak head pitch versus time, helmet 4. Peak head pitch motion for each epoch, helmet 4, 12 subjects.

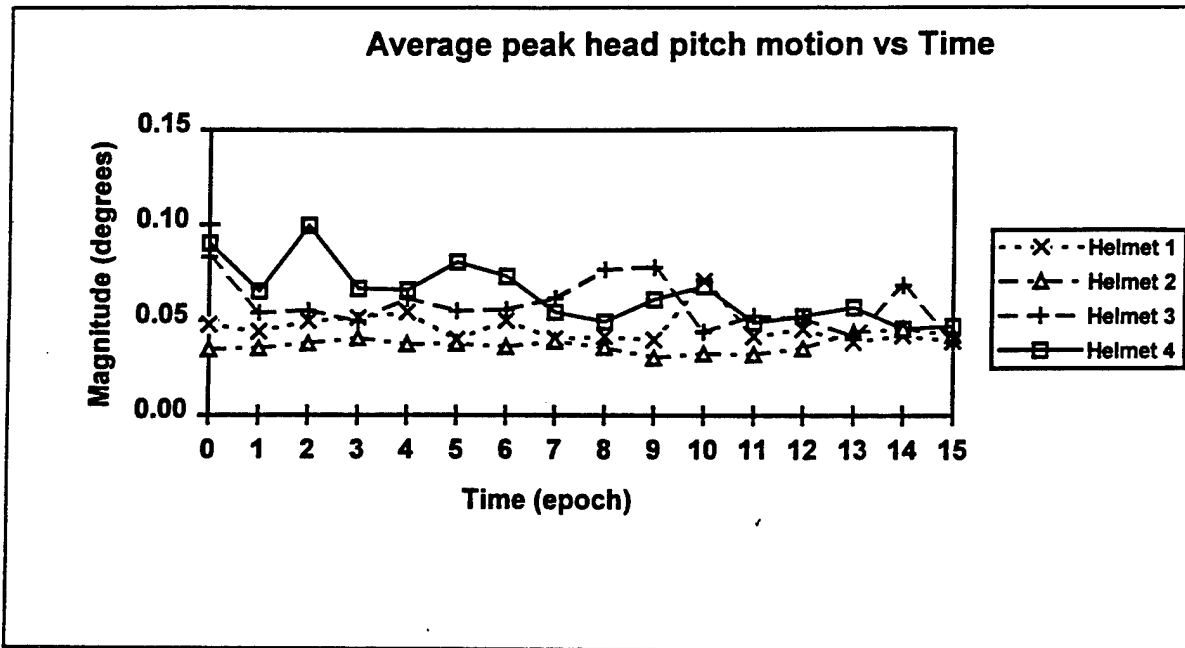


Figure 19. Average peak head pitch motion versus time. Peak head pitch motion for each epoch, helmet 4, 12 subjects.

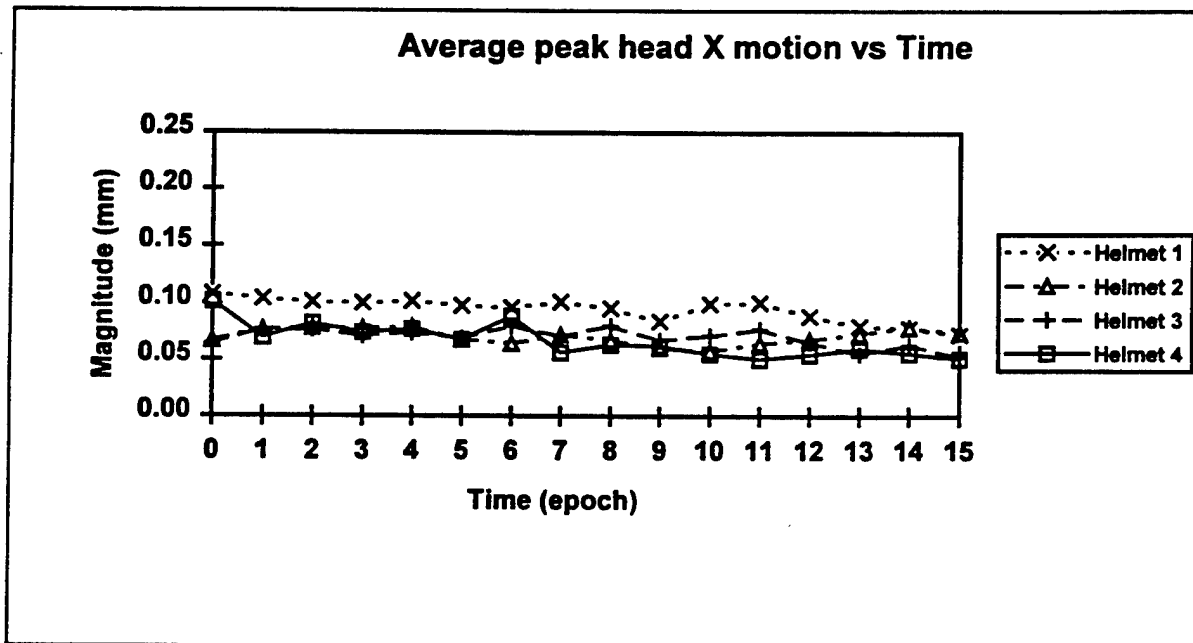


Figure 20. Average peak head X motion versus time. Peak head X motion for each epoch, four helmets, averaged by subjects.

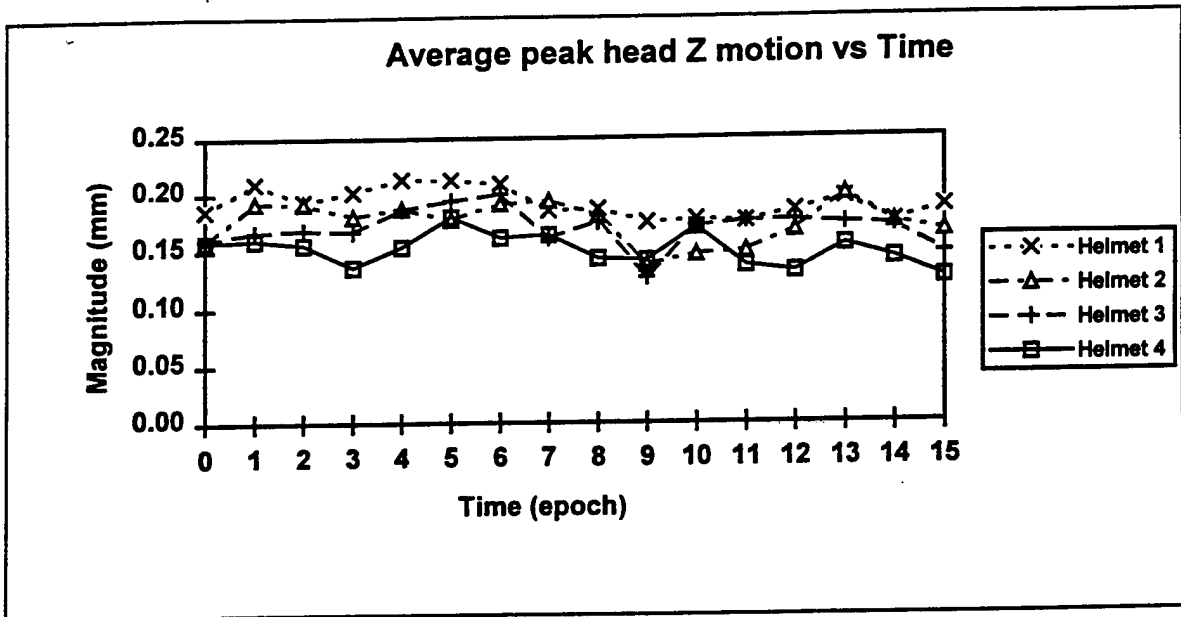


Figure 21. Average peak head Z motion versus time. Peak head Z motion for each epoch, four helmets, averaged by subjects.

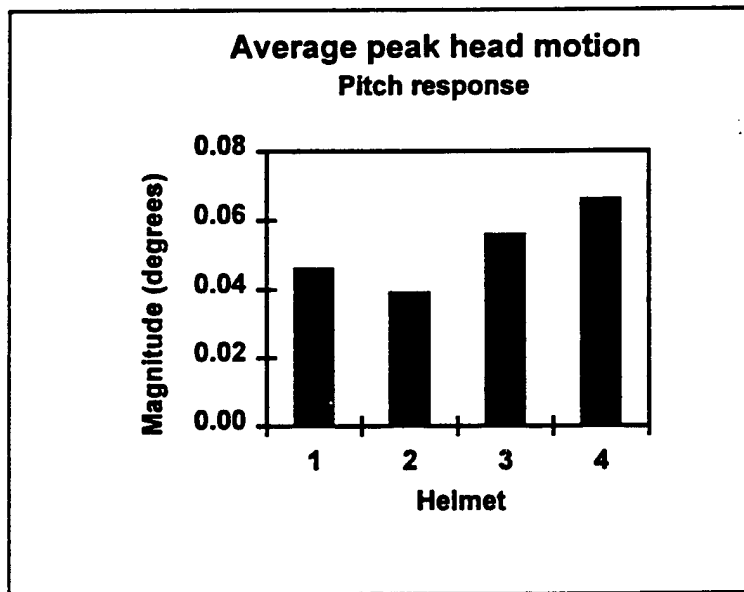


Figure 22. Average peak head pitch motion. Peak head pitch motion for helmet type averaged across epoch and subject.

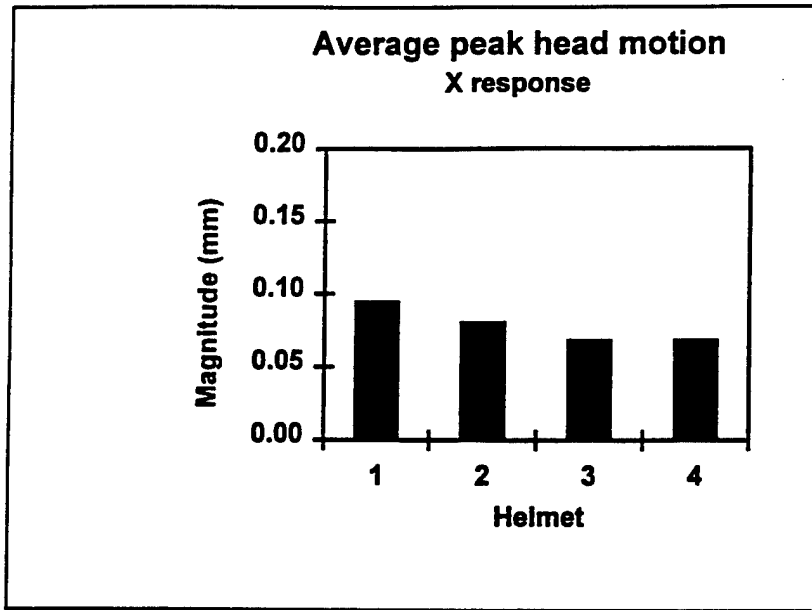


Figure 23. Average peak head X motion. Peak head X motion for helmet type averaged across epoch and subject.

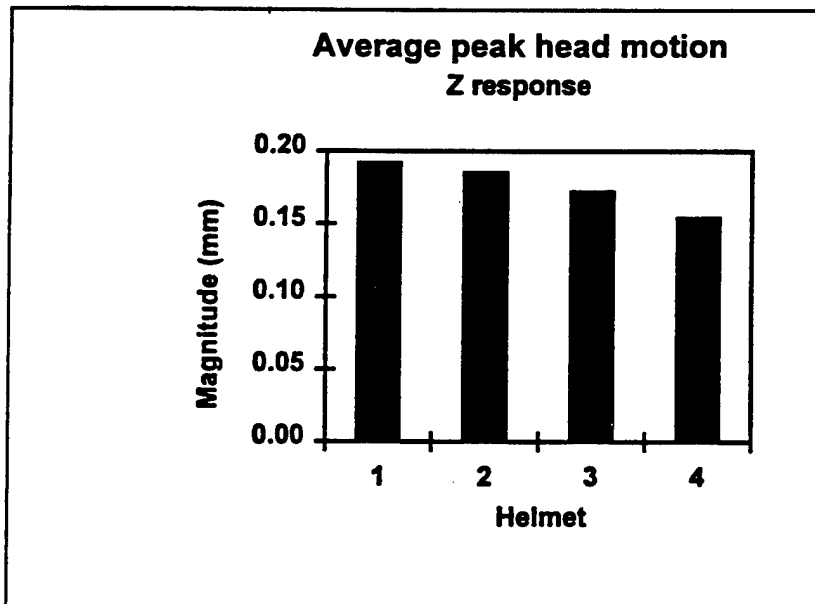


Figure 24. Average peak head Z motion. Peak head Z motion for helmet type averaged across epoch and subject.

Appendix A.

Subject briefing

Safety briefing

Mount and dismount the vibration table only when told to do so by the safety officer. Follow the safety officer's instructions at all times. This person has a safety switch that will shut down the vibration table in the unlikely event of an emergency, such as a severe vibration or jolt from the vibration table. Such an event has never occurred in the operation of the table and it is very unlikely to occur due to the many safety features of this system. If at any time you feel you want to end the testing prematurely, look at the safety officer and tell him that you want to stop the testing. The safety officer will shut down the table and you can dismount the table. Do you have any questions on the safe operation of this testing facility?

Experimental testing

You will be asked to sit on a seat on top of a vibration platform. During the main portion of the testing, you will wear a helmet and will be exposed to 4 hours of whole-body vibration. The vibration you will experience is similar to that experienced by a crewmember of a U.S. Army UH-60 helicopter.

This is a long test. There will be a 10-minute break during the test at the end of the second hour of the 4-hour vibration exposure. Before and after the vibration, you will do a series of neck muscle exertions. During the neck muscle exertions and while you are being vibrated, myoelectric measurements will be taken from the muscles around your neck. To obtain these measurements, electrodes will be placed on your skin over six of the muscles of your neck. These electrodes measure the electrical activity in your muscles. Measurements of your posture also will be taken during the vibration exposure. To obtain these measurements, markers will be placed on your skin and clothing. In preparation for placement of the electrodes and markers, your skin will be rubbed with an alcohol pad to remove a fine layer of dead skin. You may experience some redness due to the rubbing of your skin, but this should clear up in about a day.

During the vibration, you will be asked to sit in a relaxed posture. You will repeatedly do a series of performance tasks that vary in duration. There are three different types of performance tasks: target tracking, vigilance, and cognitive performance tests.

Tracking

For the tracking task, you will move your head as needed to keep the light beam mounted on your helmet on a target on a moving board in front of you. Whenever your light beam moves off the target, the amount of error will be recorded by a computer.

Vigilance

For the vigilance task, you will move your head as needed to locate targets in front of you when they light up. The target lights will turn off when you aim the light beam on your helmet at the target. The amount of time you take to turn off the targets will be recorded by a computer.

Synthetic work environment

The cognitive performance task consists of four simultaneous tasks which will last for 7 minutes. The four tasks will appear on the screen of the computer placed directly in front of you and you will enter your responses using a track ball and track ball buttons. The computer will record the score, the amount of time it took you to give an answer, and whether the answer was correct. You will be required to practice these tests 10 times prior to your participation in the vibration part of this effort. The four tasks are: a seven letter recognition task, an auditory recognition task, a three column addition task, and a position discrimination task. You have to do all four tasks at the same time. I will now describe these tasks.

In the seven letter recognition task, seven target letters are briefly presented in the top left of the screen at the start of the task. You must remember these letters. These letters will go away and you will be presented with a single letter. You must indicate with the track ball cursor and button if this letter is in the set of letters you saw at first. Letters will be presented during the test. You must watch for them and respond as best you can. You will be given 10 points for each letter you correctly identify as being in the target set, and you will lose 10 points for each letter you indicate is in the target set but is not. You must watch and listen for the other tasks while you perform this one.

In the auditory recognition task, two tones are presented: a high pitch tone and a low pitch tone. There are more low pitch tones as compared to high pitch tones. If you hear a high pitch tone, you must move the cursor to the lower right of the screen and click the track ball button indicating a high pitch tone was presented. You must listen for the tones and respond as best you can. You will be given 10 points for each correctly identified high pitch tone, and you will lose 10 points for each low tone you identify as a high pitch tone. You must watch for the other tasks while you perform this one.

In the three column addition task, you will be required to add two numbers. You will use the track ball cursor and the buttons to create a sum. For each column, click the button to increase or decrease the sum digit. When you have completed the addition, click on the box indicating you

are finished. You will receive 10 points for each correct sum, and lose 10 points for each wrong answer. You must watch and listen to the other tasks while you perform this one.

In the position discrimination task, you must watch a drifting bar approach one end of a region. The bar starts out at the middle of the region and will drift one way or the other. It will drift in only one direction once it has started. The closer you let the bar get to one end of the region, the more points you will receive. You can score as many as 10 points for each drifting bar. If the drifting bar reaches the end of the region, you will lose 10 points. Move the cursor using the track ball and click on the reset box when you want to reset the drifting bar back to the middle of the region. You must watch and listen to the other tasks while you perform this one.

Do you have any questions on the experimental procedure?

Appendix B.

Medical screening form

1. Name _____
Last First MI

2. SSN _____

3. Age _____

4. Date of last Physical Exam _____
Month Year

5. Type of Physical Exam
Class ___ I, ___ IA, ___ II, ___ III,
___ Army Entrance Physical
___ Other
___ Don't know

6. Do you have, or have you ever had, any of the following:

	Yes	No	Don't Know
a. High blood pressure	—	—	—
b. Heart problems	—	—	—
c. Broken bones within last 6 months	—	—	—
d. Muscle spasms	—	—	—
e. Back pain	—	—	—
f. Sprained or strained neck	—	—	—
g. Arthritis	—	—	—
h. Episodes of dizziness	—	—	—
i. Episodes of muscle weakness	—	—	—
j. Headaches	—	—	—
k. Whiplash	—	—	—

7. Physical activities

a. Are you actively engaged in any physical training program?
___ yes ___ no

If so, how many hours per week do you spend in the any of the following activities?

Run or jog _____
Swim _____
Tennis _____
Softball _____
Work with weights _____
Football _____
Basketball _____
Aerobics _____
Others _____

Please describe other physical activities you participate in:

b. How many hours have you flown in a military aircraft while wearing a helmet in the last month? ___ hours

Please divide the hours into each aircraft:

___ UH-1, ___ UH-60, ___ OH-58, ___ AH-64, ___ CH-47, ___ Other

c. Do you ride a motorcycle or moped? ___ yes, ___ no

If so:

Do you wear a helmet ___ yes, ___ no

How many miles do you ride per week? ___ miles

d. Do you perform any exercises specifically to strengthen the neck muscles? ___ yes, ___ no

If so, what kind?

FFD/NFFD

Medical Monitor

Date

Appendix C.

Multiaxis ride simulator

1. The MARS consists of the following equipment:
 - a. Two large hydraulic pumps in parallel, each pumping hydraulic oil at 85 gpm at up to 3600 psi for an operating pressure of 3000 psi.
 - b. Three hydraulic accessory modules for switching the hydraulic oil flow to the actuators.
 - c. Three 13.1 kip translational hydraulic actuators each having a 3-stage valve system.
 - d. Three failsafe valves, each valve capable of shutting down oil flow to the actuators within 20 msec of the command "FAILSAFE."
 - e. One multichannel servo controller (Schenck/Pegasus 5900).
2. The MARS capabilities and specifications are as follows:
 - a. Up to 600 lbs test load, including the test subject.
 - b. Frequency response: 5 to 40 Hz, flat about 0 ± 1 dB.
 - c. Up to 4 G peak acceleration.
 - d. Up to 3.5 inches peak displacement.
 - e. Failsafe shutdown occurs within 20 msec of "FAILSAFE" command from any of the following monitored parameters:
 - (1) External paddle switches.
 - (2) External safety switches on 5900 servo controller.
 - (3) AC power interrupt.
 - (4) Preset limit exceeded.
 - (5) Anticipation circuit.
 - (6) Data signal/reference signal comparison.

- (7) Accelerometer loss.
- (8) Inner or outer loop LVDT signal loss.
- (9) Safety Officer activates failsafe switch.

3. The excitation of the MARS is accomplished as follows: A command signal is applied to the first stage of the 3-stage valve for the excited axis. The first stage consists of a force motor which is a pendulum secured within the field of the force motor transformer. When excitation is applied in the form of a command signal, the pendulum moves back and forth across two openings porting oil that is proportional to the excitation. The oil thus ported is used to move a spool valve which, in turn, ports oil at the operating pressure to move the hydraulic actuator ram. The movement of the ram is proportional in direction and phase of the excitation, and in displacement to the amplitude of the excitation.

4. Excitation to the MARS actuators is output through the multichannel servo controller from the iterated transfer function controller (ITFC) computer and created as follows: The ITFC differs from a normal control system in that the reduction of the control error is not carried out on-line, but is carried out iteratively over a specified time using the desired command signal. The actuator command signals are not corrected immediately after the occurrence of a control error. They are corrected off-line on the basis of a comparison between the recorded achieved response signals and the recorded desired response signals. The calculations of the corrected drive signals are carried out by transforming the control error with a Fourier transform and then multiplying it with the corresponding elements of an inverted frequency domain response function matrix. The result of this operation is a set of correction signals in the frequency domain that is passed through an inverse Fourier transform to create a time domain signal. This signal is weighted and added to the previous iterated drive signal. This new signal is then passed through the iterative process until the desired error limits are achieved.

5. Acquisition, identification, iteration, manipulation, and output of signals are accomplished by a set of versatile software packages run by the ITFC computer. In addition to the MARS control, the ITFC can be used to analyze test data or to generate drive signals internally. Most drive signals are provided for by sampling actual vibration signals from various ground vehicles or aircraft.

Appendix D.

Statistical tables.

Table D-1.

Two-way analysis of variance for epoch and helmet.

Head pitch motion					
Source	Sum of squares	DF	Mean square	F-ratio	P
Epoch	0.023	15	0.002	1.036	0.416
Helmet	0.073	3	0.024	16.442	0.000
Epoch* helmet	0.061	45	0.001	0.914	0.635
Error	0.952	640	0.001		
Dep var: peak, N: 704, multiple R: 0.378, squared multiple R: 0.143					

Table D-2.

Two-way analysis of variance for epoch and helmet.

Head X motion					
Source	Sum of squares	DF	Mean square	F-ratio	P
Epoch	0.032	15	0.002	1.086	0.366
Helmet	0.090	3	0.030	15.278	0.000
Epoch* helmet	0.038	45	0.001	0.432	1.000
Error	1.262	640	0.002		
Dep var: peak, N: 704, multiple R: 0.338, squared multiple R: 0.144					

Table D-3.
Two-way analysis of variance for epoch and helmet.

Head Z motion					
Source	Sum of squares	DF	Mean square	F-ratio	P
Epoch	0.106	15	0.007	1.782	0.034
Helmet	0.153	3	0.051	12.839	0.000
Epoch* helmet	0.069	45	0.002	0.385	1.000
Error	2.536	640	0.004		
Dep var: peak, N: 704, multiple R: 0.338, squared multiple R: 0.114					

Table D-4.
Significant Tukey tests comparing helmets for each epoch.

Head pitch motion (* = significant differences)					
Epoch	Helmet				P
	1	2	3	4	
0		*	*		0.049
0		*		*	0.012
1		*		*	0.005
2		*		*	0.029
6		*		*	0.019

Table D-5.
Significant Tukey tests comparing helmets for each epoch.

Head X motion (* = significant differences)					
Epoch	Helmet				P
	1	2	3	4	
11	*			*	0.046

Table D-6.

Significant Tukey tests comparing helmets for each epoch.

Head Z motion (* = significant differences)					
Epoch	Helmet				P
	1	2	3	4	
3	*			*	0.008
0		*		*	0.034

Table D-7.

Significant Tukey tests comparing helmets, pooled across epoch.

Head pitch motion (p values)				
Helmet	1	2	3	4
1	1.000			
2	0.229	1.000		
3	0.034	0.000	1.000	
4	0.000	0.000	0.051	1.000

Table D-8.

Significant Tukey tests comparing helmets, pooled across epoch.

Head X motion (p values)				
Helmet	1	2	3	4
1	1.000			
2	0.009	1.000		
3	0.000	0.035	1.000	
4	0.000	0.038	1.000	1.000

Table D-9.

Significant Tukey tests comparing helmets, pooled across epoch.

Head Z motion (p values)				
Helmet	1	2	3	4
1	1.000			
2	0.710	1.000		
3	0.010	0.175	1.000	
4	0.000	0.000	0.028	1.000

Appendix E.

Glossary

Anatomical axes. The X, Y, and Z-axis located in the Frankfort plane midway between the right and left trigion. X proceeds out the bridge of the nose, Y proceeds out the left ear, and Z proceeds out the top of the head. For this study, the anatomical axes have been moved to the AO complex using the same orientation, and parallel to the Frankfort plane.

Atlanto-Occipital (AO) complex: The pivot point of the head at the top of the cervical spine. The AO complex is a multifaceted joint involving the base of the skull or occiput, the first cervical vertebra, and the second cervical vertebra. The occiput and the first cervical vertebra create a joint that is primarily responsible for head rotation about the Y-axis, or as in nodding the head Ayes.

Center-of-mass. A point about which a body's linear moments sum to zero, or the point where a body is balanced in the gravity field.

Coordinate axis. The reference axis will be defined as positive X forward, positive Y to the left, and positive Z vertical. Pitch is rotation about the Y-axis. Roll is rotation about the X-axis. Yaw is rotation about the Z-axis.

External auditory meatus (EAM). The external part of the ear canal; the part you can see.

Frankfort plane. A plane through the right and left trigion and the crest of the bony structure at the lower edge of one of the eye sockets. This defines the anatomical plane of the head.

Head-supported mass. A generic term describing any object supported by, or worn on, the head. Examples include a helmet, night vision goggles, chemical mask, oxygen mask, sun visor, etc.

Head pitch acceleration is rotational acceleration about the Y-axis.

Long-duration exposure or flight. 4 hours.

Mass. In a physics sense it is a measure of a body's resistance to acceleration. It is different from, but proportional to a body's weight.

Moment. A perpendicular force at a specified distance from a point resulting in rotational forces about that point.

Newton-centimeter (N·cm). Units describing a moment.

Reference axis. The X, Y, and Z-axis at any anatomical location, but referenced to the gravitational field where X is oriented dorsal to ventral (forward), Y is oriented lateral right to left, and Z is oriented inferior to superior (up).

Short-duration exposure or flight. 20 minutes.

Tragion. The fleshy knob of cartilage and skin just forward and centered on the EAM.

Weight moment. The static moment in the gravity field. A torque caused by the effect of gravity on a mass through a lever arm.

Whole-body vibration. Vibration experienced by the entire body as contrasted to segmental vibration where vibration is applied to a single point or limb. The usual input to whole-body vibration is the feet when standing, and the buttocks when sitting.

Appendix F.

List of abbreviations

ANOVA	analysis of variance	MVC	maximum voluntary contraction
AO	atlanto-occipital	N·cm	Newton·centimeter
AP	anterior to posterior	NVG	night-vision goggles
cm	centimeter	sec	second
dB	decibel	SWE	synthetic work environment
DFT	discrete Fourier transform	T1	first thoracic vertebrae
EEG	electroencephalography	USAARL	U.S. Army Aeromedical Research Laboratory
EMG	electromyography		
FLIR	forward looking infrared		
G	gravity		
HUD	head-up display		
Hz	hertz		
kg	kilogram		
LED	light-emitting diode		
m	meter		
MARS	multiaxis ride simulator		
mm	millimeter		